Department of Experimental Oncology

Regina Elena National Cancer Institute

Doctorate Program in "Genetics and Cellular Biology"

(XXIV cycle – 2008-2011)

Coordinator: Prof. Giorgio Prantera

"HIPK2 Controls Cytokinesis through Histone H2B Phosphorylation at the Midbody"

(BIO/18)

Prof. Giorgio Prantera

Dr. Silvia Soddu

***Ph.D. Student**: Alice Moncada*

INDEX

INDEX 1

ABSTRACT 3

INTRODUCTION 5

HIPK2 5

The cell cycle 11

Different stages of mitosis 12

Cytokinesis, the final step of Mitosis 14

Cytokinesis failure 18

RESULTS 21

HIPK2 Localizes with Histone H2B at the Midbody 21

HIPK2 Binds H2B and Phosphorylates it at S14 30

HIPK2 and histone H2B Localize at the Midbody Independently of the Presence of Chromosome Bridges 33

HIPK2 is Required for Faithful Cytokinesis 36

HIPK2 is Required for H2B-S14 Phosphorylation at the Midbody 40

HIPK2-mediated H2B-S14 Phosphorylation is Required for Cytokinesis 41

DISCUSSION 44

A DDR-Independent Interaction of HIPK2 and H2B 44

An Extra-Chromosomal Activity of H2B 45

HIPK2 in the Control of Cytokinesis 48

HIPK2 as a Tumor Suppressor 49

TABLE S1 51

EXPERIMENTAL PROCEDURES 52

Cells, Culture Conditions, and Vaccinia Virus Infection 52

GST Pull-down, Electroforesis, and Mass Spectrometry 52

Expression Vectors and Transfection 53

Immunofluorescence Microscopy 54

Western Blot, Immunoprecipitation, and Kinase Assay 54

Midbody Isolation and Extraction 55

GST Pull-Down and in Vitro Binding Assay 56

RNA Interference, RNA Extraction, and Quantitative Real-time RT-PCR 56

Live Cell Imaging 57

Statistical Analysis 57

REFERENCES 58

ABSTRACT

The homeodomain interacting protein kinase 2 (HIPK2) is a multi-talented S/T kinase playing critical role in cell fate decision during development and in DNA damage response (DDR). Here we show that HIPK2, together with its novel phosphorylation target, histone H2B, is critically involved in the final steps of cytokinesis and its inactivation promotes tetra- and poly-ploidization. Starting from a mass–spec-based identification of H2B as HIPK2 interacting protein, we demonstrated that HIPK2 binds and phosphorylates H2B at S14 (H2B-S14^{P}) and both proteins localize at the midbody during cytokinesis. The midbody localization of HIPK2 and H2B-S14P is independent of the presence of chromatin in the cleavage plane, indicating a distinct role from the DDR activities of both HIPK2 and H2B proteins. Microscopic studies and live-cell imaging with HIPK2-proficient and -defective cells revealed that HIPK2 is not necessary for the midbody localization of H2B but is required for its S14 phosphorylation in this subcellular compartment. Furthermore, we discovered that HIPK2-deficiency prevents cell cleavage, leading to regression of the cleavage furrow and accumulation of bi- and multi-nucleated cells; alternatively, it causes persistence of the connections between daughter cells with the formation of LIBs and syncytia-like structures, supporting a main role of HIPK2 in abscission. We rescued all the observed cytokinesis defects by restoring wild-type HIPK2 expression in *Hipk2*-/- mouse embryo fibroblasts (MEFs) and, most strikingly, by expressing a phosphomimetic H2B-S14D derivative, thus showing that H2B-S14^{P} is required for a faithful cytokinesis. Overall, our data point at the HIPK2/H2B interplay as an important regulator of the

final step of cell division and uncover a novel HIPK2 function in the prevention of tetraploid cell formation.

INTRODUCTION

HIPK2

The serine-threonine kinases of the Homeodomain Interacting Protein Kinase (HIPK) family have been identified among the enzymes able to regulate gene transcription. The HIPK family includes four serine-threonine kinases, numbered 1to 4, which are highly conserved in vertebrates (Kim et al., 1998).

HIPK1, HIPK2 and HIPK3 were originally discovered in a yeast two-hybrid screening with the Nkx-1.2 homeoprotein and show a conserved protein structure with more than 90% homology in the kinase domain and about 70% in the homeobox-interacting domain. These kinases can either interact with homeobox proteins and act as transcriptional corepressors, or with other types of transcription factors and act as coactivators or corepressors, depending on the promoters or the cellular context. HIPK2, the best characterized of the family, plays important roles in the regulation of proliferation and apoptosis during development and in cell response to DNA damage (reviewed Rinaldo et al., 2007a). HIPK2 was show to phosphorylate itself in vitro and binds and phosphorylates a still enlarging body of targets, including transcriptional regulators (D'Orazi et al., 2002; Hofmann et al., 2002; Zhang et al., 2003; Wiggins et al., 2004; Wee et al., 2008; Hikasa et al., 2010), chromatin modifiers (Zhang and Wang 2007; Bracaglia et al., 2009), signal transducers (Kanei-Ishii et al., 2004; Ritterhoff et al., 2010), and E3 components of SUMO ligases (Roscic et al., 2006; Swarup and Verheyen, 2011) (**Figure 1**).

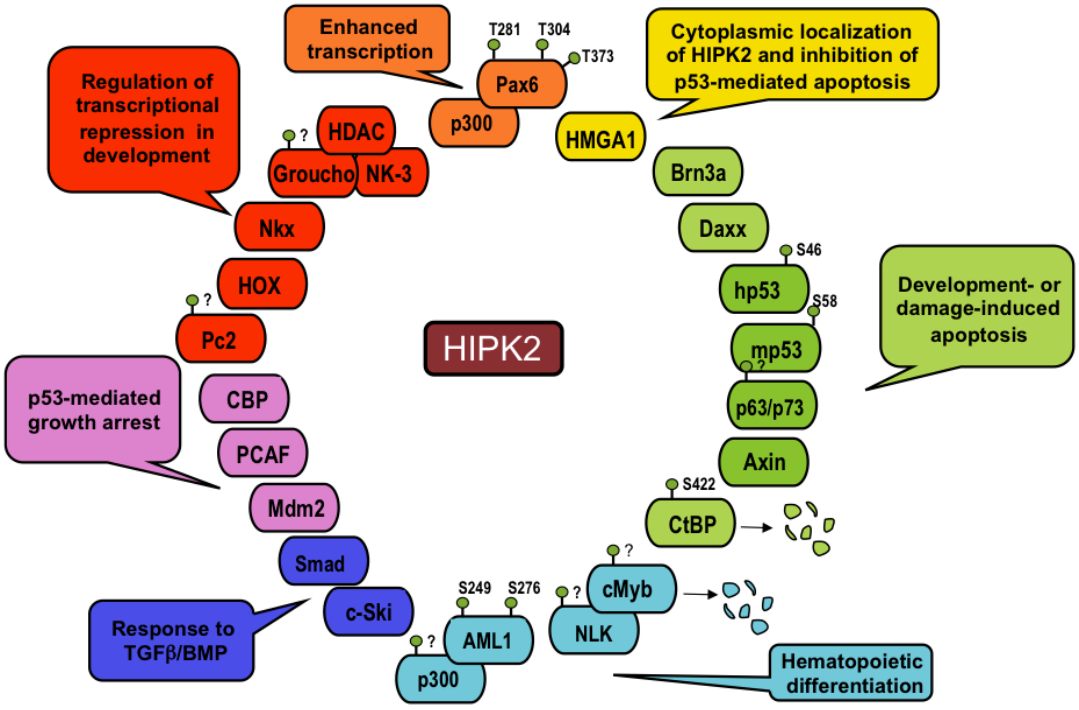


Figure 1. Schematic representation of HIPK2 targets

The protein that were shown to interact with HIPK2 are reported together with their respective biological activities. The known sites of HIPK2-induced phophorylation are indicated.

The structure of HIPK2 (1189 aa) is characterized by an N-terminal region containing a sumoylation site and a kinase domain (KD) followed by a homeobox-interacting domain (HID), a PEST-sequence containing region (rich in Proline, Glutamic acid, Serine and Threonine) and a C-terminal region that includes a speckle-retention signal (SRS), a putative autoinhibitory domain (AID), and an ubiquitylation site (**Figure 2**).

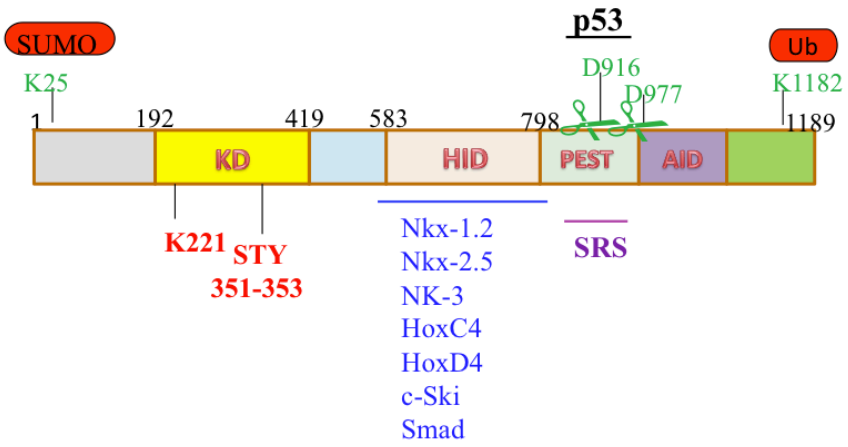


Figure 2. Schematic representation of murine HIPK2 protein

The horizontal lines outside the HIPK2 box indicate the known interacting regions of the indicated HIPK2 partners. K25 is the sumoylation site; KD is the kinase domain in which K221 is the catalytic site, and STY is the activation loop. HID is the omeobox-interacting domain, PEST is PEST-sequence- containing region, D916 and D977 are the caspase cleavage sites, SRS is the speckle-retention signal, and K1182 is the ubiquitylation site.

The kinase domain is a p38MAPK-like domain highly conserved among the members of the HIPK family and through evolution. The K221 catalytic site and the so-called activation loop (STY) are consensus motifs present in the kinase domain of the DYRK (dual specificity tyrosine-(Y)-phosphorylation regulated kinase) subfamily that includes proteins present in Drosophila and yeast. In addiction to the putative activation loop STY, two post translational modification sites have been defined and characterized in the HIPK2 protein: the sumoylation site at Lys 25 (Gresko et al., 2005; Hofmann et al., 2005; Sung et al., 2005) and the ubiquitylation site at Lys 1182 (Rinaldo et al. 2007). Sumoylation was found to regulate both HIPK2 activation and activity on target factors, while ubiquitylation has been involved in HIPK2 inactivation. In particular, upon DNA damage, HIPK2 phophorylates its own E3 SUMO ligase Pc2, which in turn triggers HIPK2

sumoylation, establishing a positive feedback loop that enhances the HIPK2 ability to act as a transcriptional repressor (Gresko et al. 2006). In contrast, HIPK2 ubiquitylation at the C-terminus is mediated by the E3 ubiquitin ligase MDM2 and promoted HIPK2 degradation via the proteasome (Rinaldo et al., 2007). Indeed, HIPK2 apoptotic activity is increased upon deletion of the region critical for MDM2-mediated degradation. Consistent with this model, a degradation-resistant HIPK2-KI182 mutant has increased apoptotic activity (Rinaldo et al., 2007).

HIPK2 exerts its effects on DDR by binding and phosphorylating an increasing array of transcription factors and coregulators. The p53 tumor suppressor is among the first non-homeotic transcription factors identified as HIPK2 target. Indeed, HIPK2 interacts through its SRS with the C-terminus of p53 and regulates its localization, phosphorylation, acetylation, and transcriptional activity. HIPK2 and p53 colocalize into the nuclear bodies together with the promyelocytic leukemia protein IV (PML-IV) and cooperate in the activation of p53-dependent transcription and induction of apoptosis (D'Orazi et al., 2002, Hofmann et al., 2002). HIPK2 activity enhances the p53-mediated transcriptional activation of pro-apoptotic factor such as PIG3, BAX, and NOXA, as well as the repression of the anti-apoptotic factor Galectin-3 (D'Orazi et al., 2002; Hofmann et al., 2002; Di Stefano et al., 2004; Cecchinelli et al., 2006a). In particular, upon severe DNA damage by UV irradiation or antineoplastic treatments such as doxorubicin or cisplatin, HIPK2 specifically phosphorylates human p53 at Ser46 and mouse p53 at Ser58 and this kinase activity is required for the induction of apoptosis (D'Orazi et al., 2002; Hofmann et al., 2002; Moller et al., 2003; Di Stefano et al., 2004;

Cecchinelli et al., 2006b).In addition, HIPK2 can promote apoptosis by targeting factors other than p53, such as the CtBP transcriptional co-repressor (Zhang et al., 2003), and by modulating the activity of other proteins directly or indirectly related to apoptosis, such as the p53 family members p73 and p63 (Kim et al., 2002; Lazzari et al., 2011) and the p53 inhibitor MDM2 (Wang et al., 2001; Di Stefano et al., 2004).

Reduction of HIPK2 expression by RNA-specific interference (RNAi) was shown to impair apoptosis and induce resistance to different anticancer treatments (Krieghoff-Henning and Hofmann, 2008; Puca et al., 2010), suggesting that HIPK2, like other genotoxic stress responders or apoptosis activators, is a tumor suppressor on its own. Indeed, a few mechanisms of HIPK2 inactivation have been identified in human cancers, such as HIPK2 forced cytoplasmic relocalization in breast carcinomas and in leukemogenesis (Pierantoni et al., 2007; Wee et al., 2008), HIPK2 mutations in acute myeloid leukemia (Li et al., 2007), and allele-specific loss of heterozygosity in thyroid cancers (Lavra et al., 2011). Recently, a screening for genetic alterations in radiation-induced thymic lymphomas demonstrated that *Hipk2* is a haploinsufficient tumor suppressor gene in vivo, showing loss of one *Hipk2* allele in 30% of the tumors and increased susceptibility of Hipk2+/- mice to radiation- induced thymic lymphoma (Mao et al., 2011).

During development, impaired proliferation, rather than apoptosis defects, has been observed. Hipk2-/- mice can survive and be fertile (Isono et al., 2006), but they are significantly smaller than their wild-type littermates throughout adulthood (Trapasso et al., 2009), are born at a reduced mendelian rate and proliferation

defects have been observed in sensory neurons (Wiggins et al., 2004) and in MEFs (Trapasso et al., 2009). *Hipk1*/*Hipk2* double knockout embryos die between 9.5 and 12.5 days post-coitus with proliferation defects (Isono et al., 2006), confirming a role in cell proliferation and indicating redundancy between the two members of the HIPK family. Though induction of HIPK2 expression was observed upon cell cycle reactivation of quiescent cells, including G0 peripheral blood mononuclear cells (Iacovelli et al., 2009), the function(s) and the mechanism(s) played by HIPK2 in the regulation of cell proliferation are still unknown, neither we understand whether they might contribute to the HIPK2 tumor suppressing activity.

The cell cycle

Cell reproduction is fundamental to the development and function of life. In single-cell organisms, one cell division creates two new organisms. In the development of multi-cellular organisms, countless cell divisions transform a single cell into diverse communities of cells that form the various tissues and organs that comprise the mature creatures. A series of highly regulated and coordinated events, termed the cell cycle, ensure that a cell duplicates its contents before dividing into two identical daughter cells. The duplication and division of cellular components must be achieved with extreme precision and reliability in every cycle. This is especially true for the genetic information, encoded in the chromosomal DNA, which is allowed to duplicate once and only once per cell cycle. In eukaryotic cells, DNA is replicated in S (synthesis) phase, resulting in duplicated chromosomes, called sister chromatids, that then must be equally segregated to the daughter cells during the so-called M (mitotic) phase (**Figure 3**).

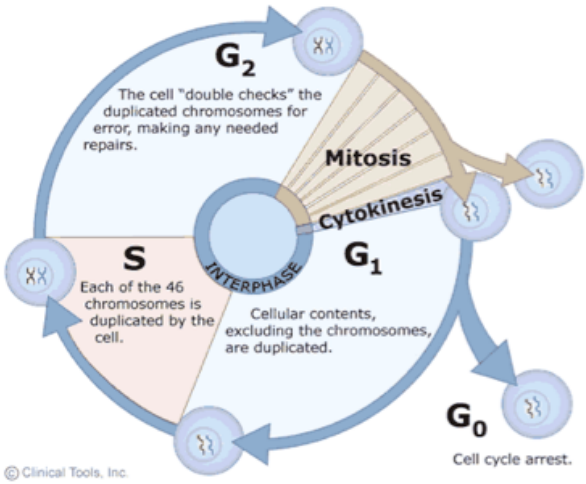


Figure 3. The eukaryotic cell cycle. Interphase consists of S, G1 (Gap 1) and G2 (Gap 2) phase. M phase is composed of nuclear division (mitosis) and cell division (cytokinesis).

Besides the DNA, a small organelle called centrosome is also duplicated once and only once per cell cycle. The centrosome cycle is tightly coupled to the cell cycle as centrosomes also replicate during S phase and migrate to opposite poles of the cell in the beginning of M phase to organize the mitotic spindle during mitosis. Upon cell division, each daughter cell receives one centrosome. As the integrity of the genome must be maintained, different cell cycle events are highly regulated by various checkpoints, thus ensuring that errors are not propagated. For example, entry into M phase is dependent on DNA synthesis, ensuring that M phase always occurs after S phase. Two gap phases (G1 and G2) respond to both positive and negative growth signals (G1) and prepare the cell for entry into mitosis (G2). An additional phase (G0) refers to a quiescent state in which the cell remains metabolically active, but no longer proliferates unless appropriate extracellular signals are received.

Different stages of mitosis

Mitosis can be subdivided into five morphologically distinct phases: Prophase, Prometaphase, Metaphase, Anaphase, Telophase and Cytokinesis (**Figure 4**). During prophase, chromatin condenses to form chromosomes consisting of two sister chromatids that are tethered together at the centromere, a specialized complex chromatin structure consisting of heterochromatic DNA. The centrosomes, which have also been duplicated during S phase, separate and migrate to opposite poles of the nucleus, thereby allowing their distribution into daughter cells at the end of mitosis. In prometaphase, after nuclear envelope break down (NEBD), specialized

structures called kinetochores (KTs) assemble on the centromeric region and are captured by microtubules (MTs), which are nucleated from the centrosomes. This capturing step happens in a highly dynamic and stochastic process. Once the KTs of the sister chromatids are attached to spindle MTs emerging from opposite poles (bipolar attachment) they are moved to the cell equator (metaphase plate) and the cell enters metaphase. After the alignment of all chromosomes at the metaphase plate, the cell enters anaphase and sister chromatids that have so far been held together by cohesin complexes are pulled apart to opposite poles. Mitosis ends with telophase, during which the mitotic spindle disassembles, sister chromatids decondense and the nuclear envelope reforms. After the formation of daughter nuclei in mitosis, cytoplasmic division (cytokinesis) divides the mother cell into two daughter cells. Finally, abscission takes place resulting in the formation of two genetically identical daughter cells.

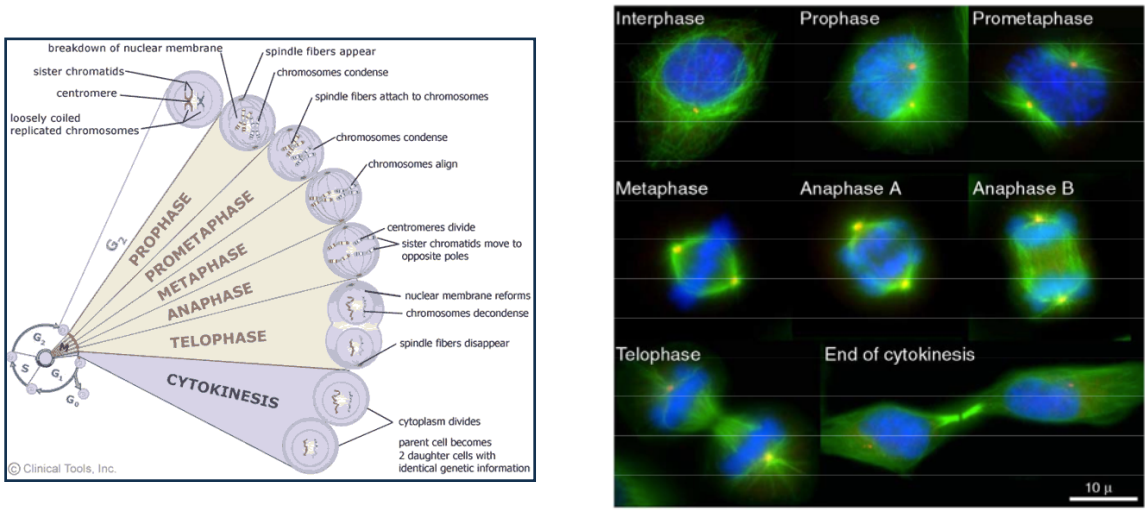


Figure 4. The different stages of M phase. The immunofluorescence images illustrate HeLa cells in different cell cycle stages. The mitotic spindle is shown in green (α-Tubulin), the centrosomes in red (γ-Tubulin) and DNA in blue (DAPI staining)

Cytokinesis, the final step of Mitosis

Cytokinesis is the final step in cell division. The process begins during chromosome segregation, when the cleavage furrow begins to partition the cytoplasm between the nascent daughter cells. The process is not completed until much later, however, when the final cytoplasmic bridge connecting the two daughter cells is severed. Cytokinesis is a highly ordered process, requiring an intricate interplay between cytoskeletal, chromosomal and cell cycle regulatory pathways. A surprisingly broad range of additional cellular factors and processes are also important for cytokinesis, including protein and membrane trafficking, lipid metabolism, protein synthesis and signaling pathways (Glotzer, 2005; Barr and Gurneberg, 2007). Three separate populations of microtubules have been implicated in the regulation of cytokinesis (**Figure 5**).

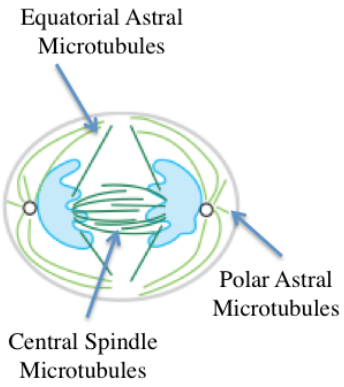


Figure 5. Three separate populations of microtubules implicated in the regulation of cytokinesis

Equatorial astral microtubules, which emanate from the spindle pole to the site of cleavage, may be stabilized in the equatorial cortical region and deliver positive signals that stimulate formation and contraction of the cleavage furrow.

Polar astral microtubules, which emanate from the spindle pole to sites away from the site of the furrow, may help position the cleavage furrow by inhibiting cortical contractility, perhaps by spatially biasing the pattern of myosin recruitment. Finally, *central spindle microtubules*, which form an overlapping network between the spindle poles following anaphase, send positive signals that become especially important during later steps of cytokinesis. The signals sent by these distinct microtubule populations are partially redundant, ensuring that selection of the division plane is robust.

The process of cytokinesis can be divided into four stages (**Figure 6**):

- Stage I: Positioning the Division Plane and Initiating Cytokinesis
- Stage II: Ingression of the Cleavage Furrow
- Stage III: Formation of the Midbody
- Stage IV: Abscission

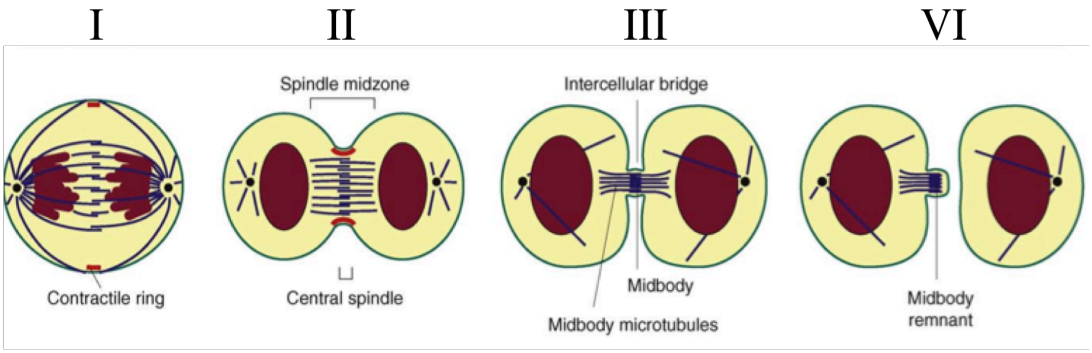


Figure 6. Multiple stages of cytokinesis.

(I) Three populations of microtubules first specify the site of cleavage by activating RhoA in a narrow zone between segregating chromosomes. **(II)** Formation and activation of the actomyosin ring next leads to furrow ingression. **(III)** The constricting furrow compacts the central spindle microtubules leading to midbody formation. **(IV)** Abscission of the furrow occurs by physically separating the cytoplasm of the daughter cells.

Each stage is dependent on the proper execution of the prior stage and thus interference with any stage may result in cytokinesis failure.

The first stage of cytokinesis begins with assembly of a central spindle during anaphase. Together with the spindle asters, the central spindle determines the position of the cleavage plane by directing localization and activation of the small GTPase RHOA at the cell cortex, which promotes assembly of a contractile actin–myosin ring and furrow ingression. If this step is perturbed, cytokinesis will not initiate properly.

In the second stage of cytokinesis, the cleavage furrow ingresses through formation of an actin-myosin ring and myosin-dependent motor activity. Several factors contribute to central spindle formation. Failure at this step may lead to a lack of furrow initiation or partial ingression of the furrow followed by regression.

The third stage of cytokinesis is characterized by formation of the midbody and stabilization of the cytokinetic furrow. As cytokinesis progresses, the constricting furrow compacts the midzone microtubule array. The furrow ingresses until a cytoplasmic bridge is formed that is 1-1.5 microns in diameter. Several kinesin-like motor proteins and chromosomal passenger proteins move along the midzone spindle towards the plus ends and accumulate in the overlapping region, forming a phase-dense structure referred to as the Flemming body, stembody, telophase disc, or midbody (**Figure 7**). Scaffold proteins such as anillin and septins may stabilize the bridge structure. In almost all systems, central spindle formation is essential for midbody formation, which in turn is necessary for abscission. A failure at this stage will lead to regression of the cleavage furrow.

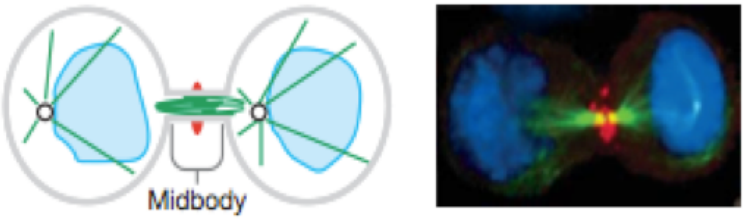


Figure 7. Schematic and immunofluorescence illustrations showing midbody

The cleavage furrow has fully ingressed compressing the midzone and creating an intercellular bridge containing a microtubule midbody. Completion occurs when the intercellular bridge is resolved creating two daughter cells. DNA (light blue), microtubules (green), and the cleavage furrow protein Anillin (red) are shown

Once the midbody is formed, it subsequently organizes the final event of cytokinesis, termed abscission. By the time of abscission, the cytoplasmic bridge has narrowed to 0.2 microns in diameter. At these late stages, microtubule bundles become compacted and begin to disappear. In this process, the cytoplasmic bridge is reorganized to permit separation of the daughter cells. A wide variety of proteins involved in vesicle and protein trafficking, membrane fusion and other processes are required for abscission, suggesting the final stage of cytokinesis is just as complex as earlier stages. Human cultured cells may remain connected by the cytoplasmic bridge for many hours before undergoing abscission. In some systems, such as embryos, blastomeres often remain connected by intracellular bridges for many cell cycles. Failure at this stage may lead to regression of the cleavage furrow or to formation of a persistent connection between the two daughter cells.

Cytokinesis failure

Cytokinesis is a surprisingly complex process that requires the interplay of many components and regulatory pathways. Cytokinesis failure can arise through defects in any of the four stages in cytokinesis. Inhibition or excessive activation of different cytokinesis components can give rise to distinct phenotypes, including precocious ingression before the chromosomes have been separated, regression of the furrow giving rise to binucleated cells, or stabilization of the cytoplasmic bridge where daughter cells remain connected (**Figure 8**).

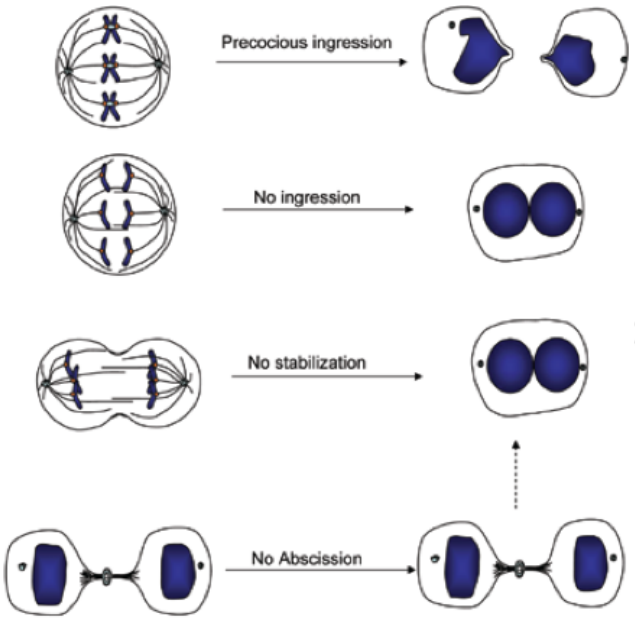


Figure 8. Summary of different phenotypes resulting from cytokinesis failure.

One possible consequence of abortive cytokinesis may be cleavage furrow regression and formation of binucleate cells. The state in which cells contain more than two sets of chromosomes is known as polyploidy. Polyploidy frequently occurs in nature and is thought to be a normal situation. Tetraploid cells are present

in normal organs such as liver and heart, whereas syncytial cells are observed in early embryogenesis and spermatogenesis (Haglund et al., 2011). However, besides these physiological conditions, cytokinesis failure and the resulting tetra- and poly-ploidization can lead to genetically unstable states and contribute to tumorigenic transformation (Fujiwara et al., 2005; Ganem et al., 2007) (**Figure 9**). In addiction, the inhibition or regression of the cleavage furrow induces persistence of connections between daughter cells with formation of long intercellular bridges (LIBs) and syncytial-like structures (Normand and King, 2010).

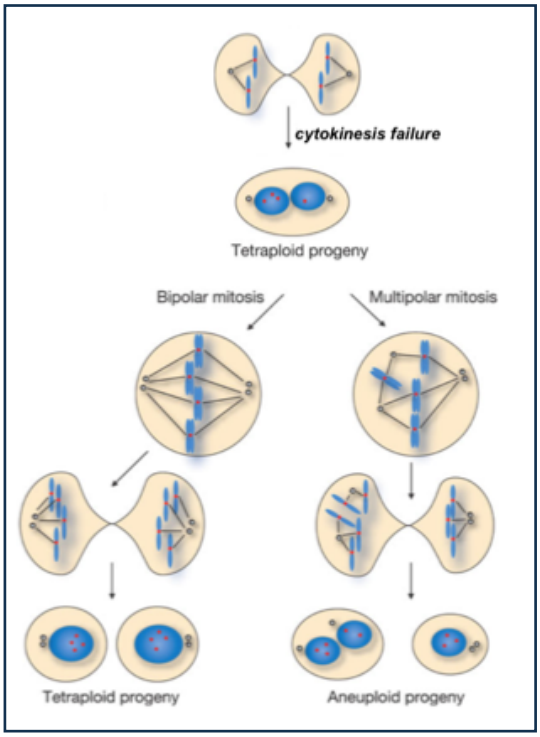


Figure 9. Model summarizing the relationship of cytokinesis failure and subsequent possible fates of resulting binucleated cells. Cytokinesis failure is associated with furrow regression, producing a binucleated tetraploid cell. If this cell divides, it can proceed through bipolar mitosis to produce two mononucleated tetraploid cells with equivalent genomes. However, if a multipolar spindle is formed, aneuploid progeny are likely to be produced due to high rates of chromosome mis-segregation resulting from multipolar mitosis.

Failures in cytokinesis can lead to tetraploidy. Faithful cytokinesis requires tight coordination with chromosome segregation (Eggert et al., 2006; Glotzer, 2005). Specifically, the completion of cytokinesis by abscission needs to await complete clearance of chromatin from the cleavage plane. While chromosome segregation normally completes early after anaphase onset, it can be severely delayed by lagging or bridged chromosomes. Such segregation defects have been estimated to occur in about 1% of dividing somatic cells, and at higher incidence in transformed cells (Cimini et al., 2003). Chromosome bridges can result from dysfunctional telomeres (Maser and DePinho, 2002; Stewenius et al., 2005), DNA double-strand breaks (Acilan et al., 2007), or from misregulated chromosome cohesion (Cimini et al., 2003) or decatenation (Chan et al., 2007). It is unclear how cells respond to chromosome bridges (Ganem et al., 2007), and if any control mechanisms would ensure faithful abscission in the presence of chromosome bridges.

RESULTS

To identify novel HIPK2-interacting factors, the full-length HIPK2 was overexpressed as eukaryotic glutathione S-transferase fusion protein (eGST-HIPK2) in human H1299 cells by a T7 vaccinia system. Cells overexpressing eGST alone were used as controls. Total cell extracts (TCEs) were subjected to GST pull-down and mass- spec analysis. In addition to already known HIPK2 targets, we identified novel HIPK2-interacting proteins such as vaccinia virus virion core protein P4b, heat shock protein 70, actin, eukaryotic translation elongation factor 1 gamma, and histones H2A/H2AX and H2B.

HIPK2 Localizes with Histone H2B at the Midbody

Because of the mostly nuclear localization of HIPK2 and its activity in DDR and apoptosis, we focused on histones H2A/H2AX and H2B. Since our lysis conditions were compatible with the maintenance of protein-protein interactions and not sufficient to efficiently extract core histones from intact DNA, we initially thought that the two co-precipitated histones might come from the apoptotic DNA usually induced by high levels of HIPK2 expression. Indeed, in their phosphorylated forms g-H2AX and H2B-S14P, these two histones are involved in DDR and apoptosis, being present at sites flanking DNA double strand breaks (DSBs) and resulting in discrete foci, critical for the recruitment of damage-signaling and repair factors or the condensation of apoptotic chromatin (Perez-Cadahia et al., 2010). Thus, we asked whether HIPK2 might interact with γ-H2AX and/or H2B-S14P at DNA

damage-induced foci. An EGFP-tagged HIPK2 was expressed in HeLa cells and its co-localization with endogenous γ-H2AX and/or H2B-S14P was assessed by immunofluorescence (IF) with anti-phospho specific antibodies (Abs), with or without γ-irradiation. No co-localization of EGFP-HIPK2 with either histone was detected at the damage-induced foci or upon the formation of apoptotic chromatin (**Figure 9**).

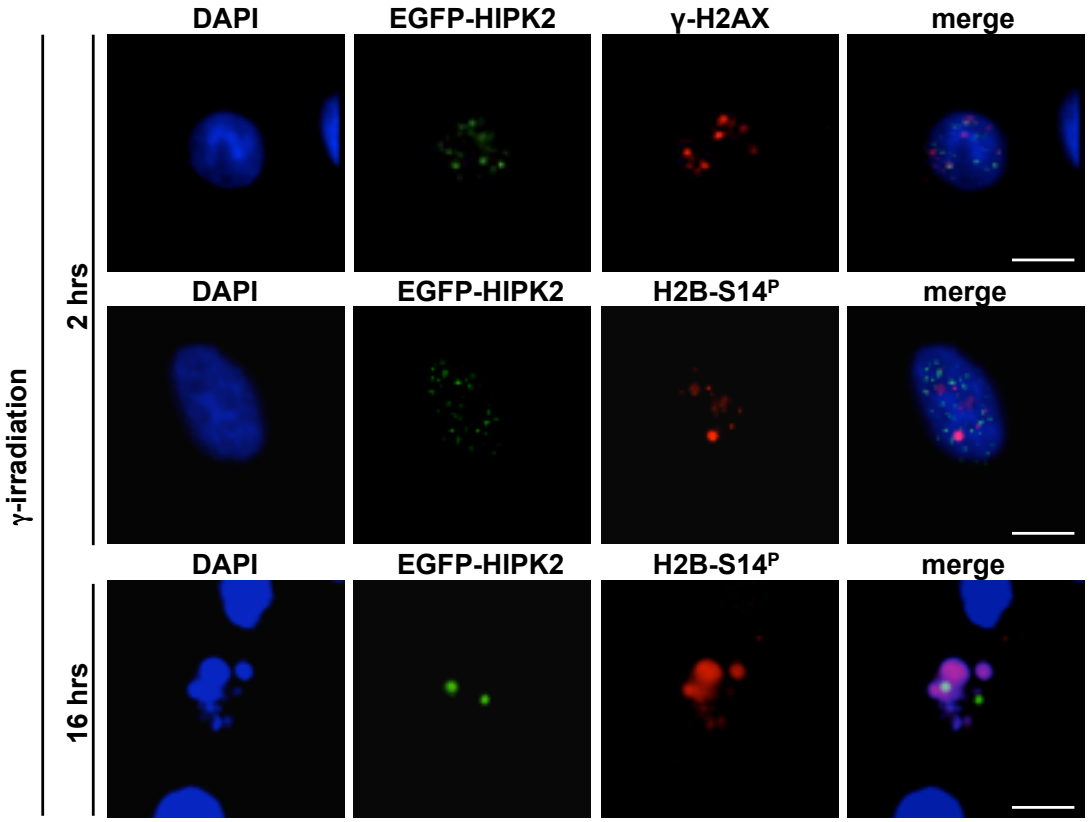


Figure 9. Localization of EGFP-HIPK2, γ-H2Ax and H2B-S14P in Irradiated Cell.

HeLa cells were transfected with EGFP-HIPK2 expressing vector and γ-irradiated (5Gy) 20hrs post-transfection. Cells were stained with anti-γ-H2Ax or anti-p-Histone H2B-S14 and DAPI to visualize DNA at the indicated times after γ-irradiation. Multiple stacks were recorded. Representative deconvolution images are shown. Here and in the following figures, Bar is 10 μm.

Surprisingly, in non-irradiated control cells, a clear localization of both EGFP-HIPK2 and H2B-S14P was observed within the intercellular bridges at the midbody, in all the telophases analyzed (n=100, **Figure 10**).

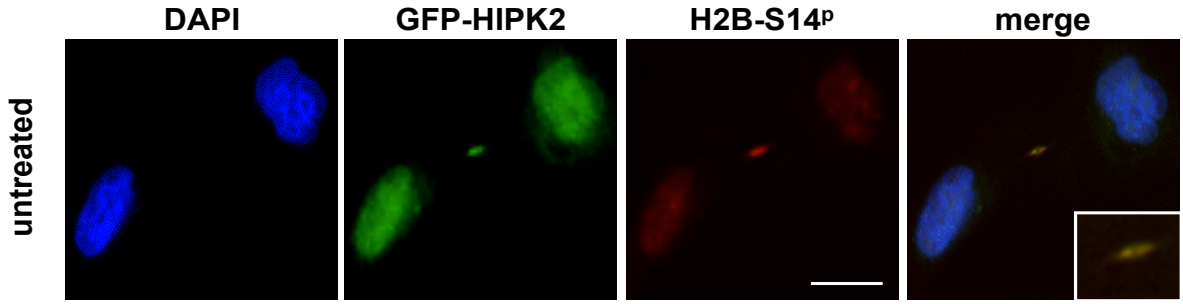


Figure 10. Localization of EGFP-HIPK2 and H2B-S14P in Control Cells

Control, untreated HeLa cells from the experiment reported above show a midbody localization of both EGFP-HIPK2 and H2B-S14P. Representative images obtained by anti-p-Histone H2B-S14 Ab are reported. Here and in the following figures, enlarged midbody region of the merge is shown in the box.

The consistency of this peculiar distribution prompted us to investigate it; we first confirmed the midbody localization of HIPK2 and H2B-S14P in different human and mouse cells by employing HIPK2 with a different tag (FLAG at the N-terminus) (**Figure 11**). Next, we verified the specificity of the H2B-S14P staining at the midbody by peptide competition and challenged the identification of endogenous H2B at the midbody by IF with anti-H2B Abs that recognize this histone independently of its posttranslational modifications (**Figures 11**, **Table S1**).

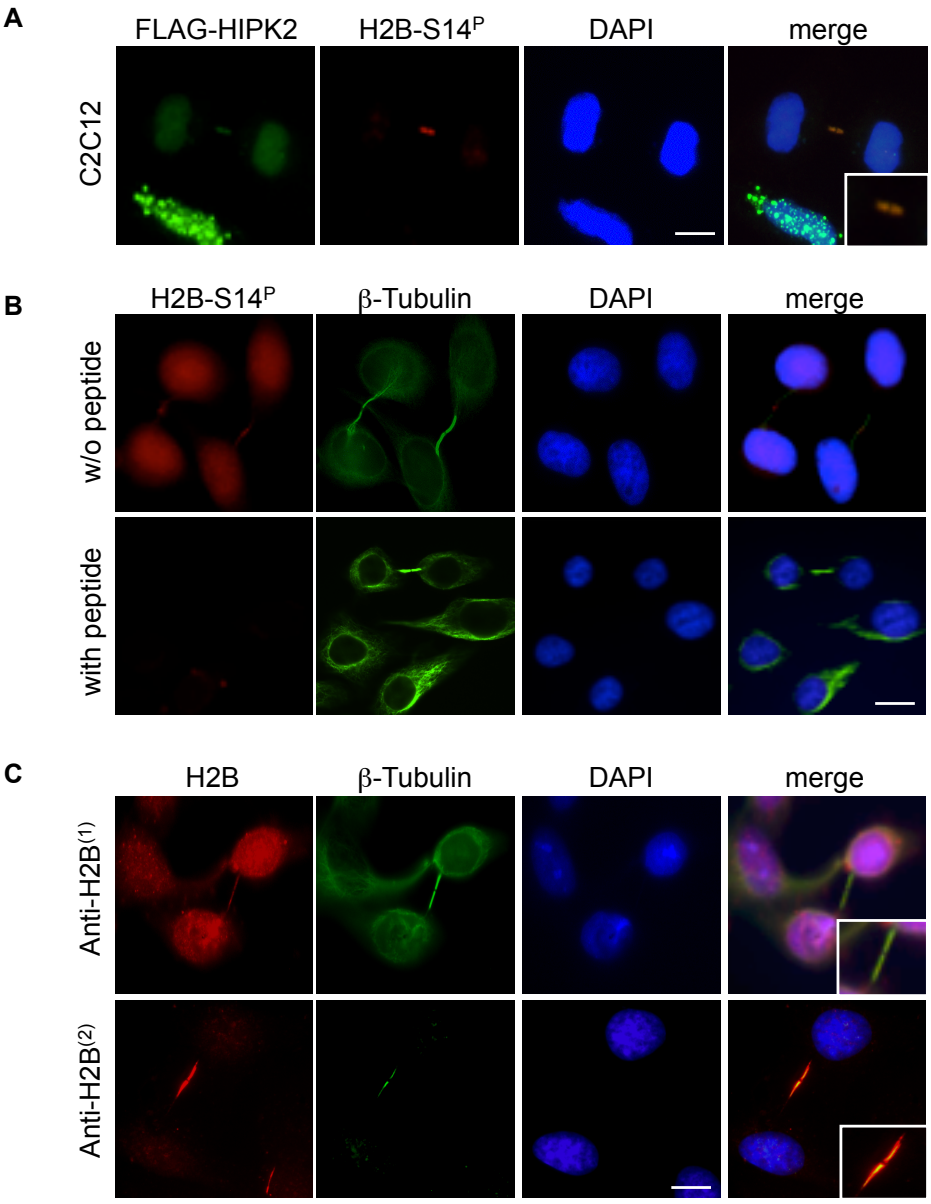


Figure 11. HIPK2 and H2B Localization at the Midbody

(A) HIPK2 and H2B-S14P co-localize at the midbody in mouse C2C12 cells. C2C12 cells were transfected with FLAG HIPK2 and stained with anti-FLAG (green), anti-p-Histone H2B-S14(1) Ab (red), and DAPI. **(B)** Competition assay for midbody staining with the anti-p-Histone H2B-S14$^{(1)}$ Ab. Immunostaining of HeLa cells was performed in the absence (upper panel) or presence (lower panel) of an excess of peptide antigen to which the anti-p-Histone H2B-S14$^{(1)}$ Ab was raised. **(C)** H2B localization at midbody during cytokineis. HeLa cells were stained with two different anti-H2B Abs (red), anti-tubulin Ab (green) and DAPI. The anti-H2B$^{(2)}$ Ab recognizes preferentially the extra-nucleosomal form of H2B. Bars are 10μm.

To assess the subcellular distribution of endogenous HIPK2, exponentially proliferating HeLa cells were fixed, subjected to antigen (Ag)-retrieval, and analyzed by IF with two different anti-HIPK2 Abs (**Table S1**). During cytokinesis, the endogenous HIPK2 protein showed clear midbody localization, whose specificity was confirmed by peptide competition (**Figure 12**).

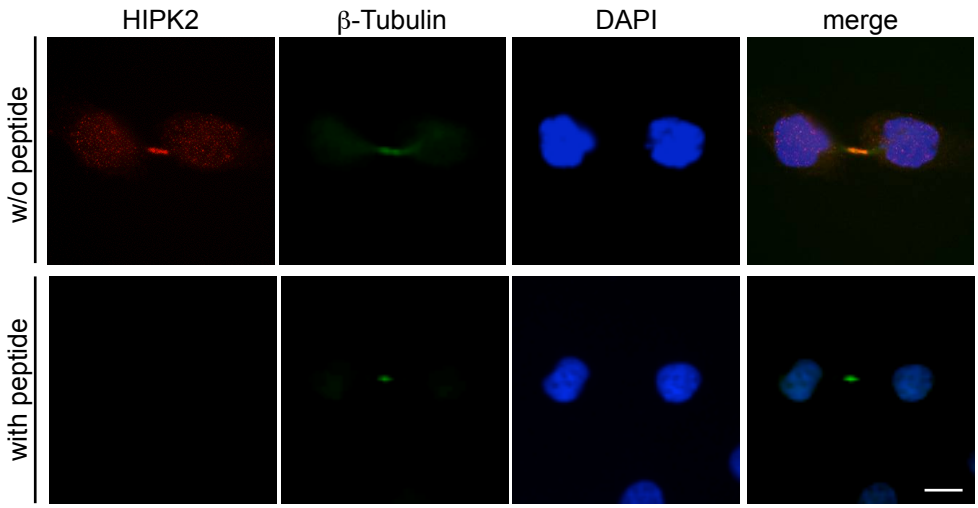


Figure 12. HIPK2 Antibody Specificity

The anti-HIPK2 specificity was demonstrated by a competition assay. Immunostaining of HeLa cells was performed in the absence (upper panels) or the presence (lower panels) of an excess of peptide antigen to which the anti-HIPK2$^{(2)}$ Ab was raised.

We could confirm the localization of HIPK2 at the midbody by employing several human and mouse cells, including tumor (HeLa, U2OS, MCF7), and non-transformed cells (C2C12, HF, AHH1), different tagged-HIPK2 proteins (EGFP or FLAG at the N- terminus and HA at the C-terminus (**Figure 13** and data not shown).

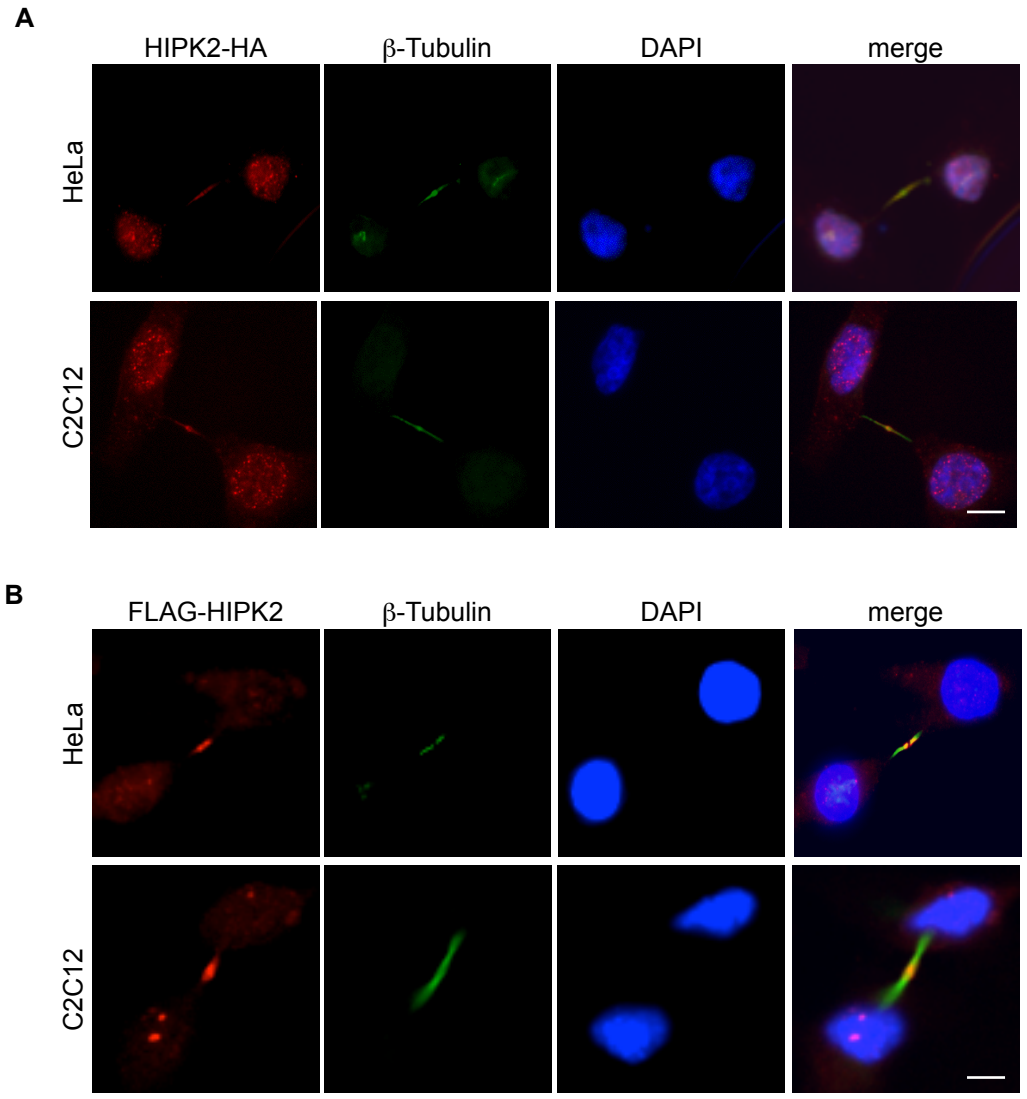


Figure 13. Exogenous HIPK2 Localization at Midbody

Different HIPK2-tagged proteins localize at the midbody in human HeLa cells and in murine C2C12. HeLa and C2C12 cells were transfected with indicated expressing vectors and stained with anti-HA **(A)** or anti-FLAG **(B)**, anti-β-tubulin Ab, and DAPI. Representative immunostaining are reported. Bar is 10μm.

In addition, we observed that both HIPK2 and H2B co-localize with well-characterized midbody markers, such as α- and β-tubulin and Aurora B kinase (Ruchaud et al., 2007) (**Figures 14**), and that these co- localizations occur at the midbody of all the telophases analyzed (n=300).

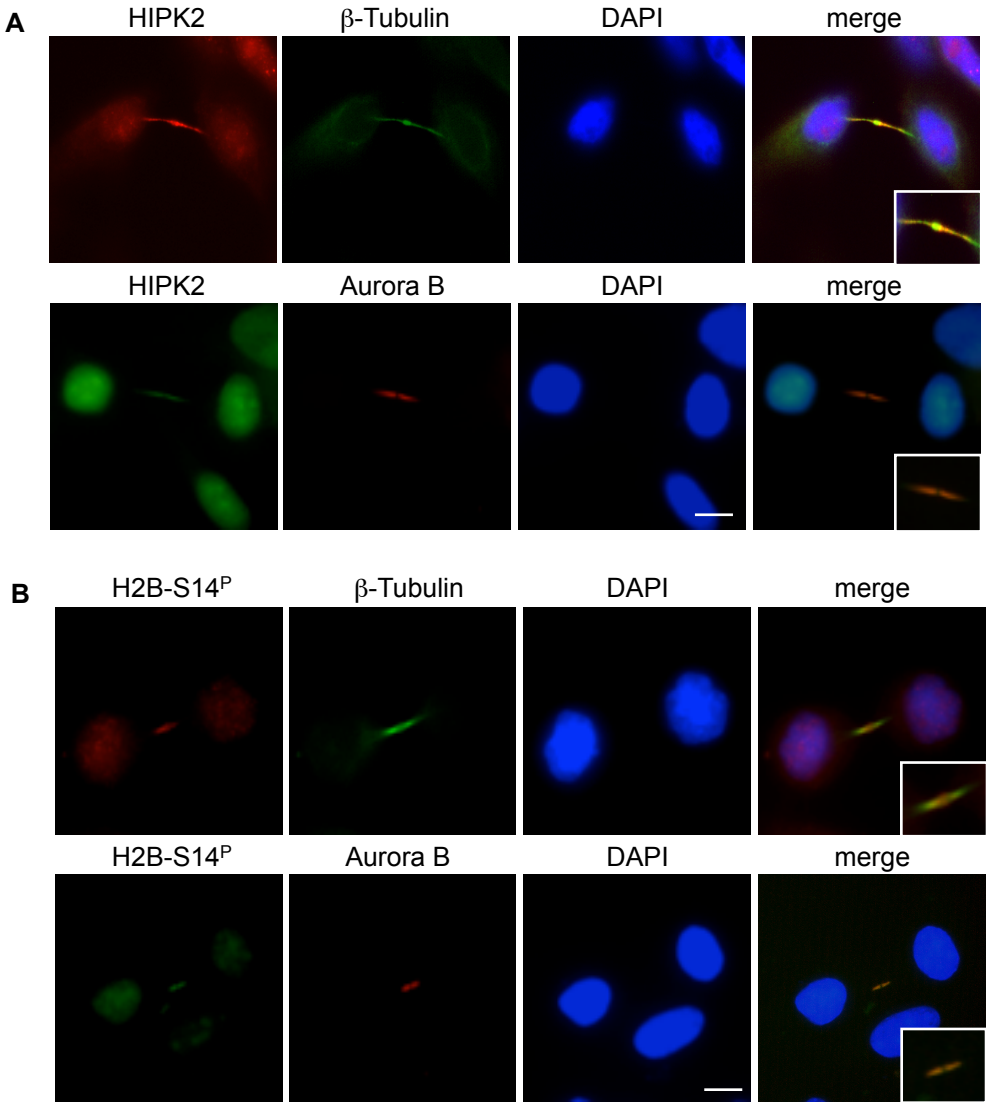


Figure 14. Localization of Endogenous HIPK2 and H2B-S14p at the Midbody

(A) HeLa cells were stained with anti-HIPK2[(1)] (red, top panel; green, bottom panel;) and anti-b-tubulin (green, top panel) or anti-Aurora B (red, bottom panel) and DAPI. Representative images are shown. **(B)** HeLa cells were stained with anti-p-Histone H2B-S14 (red, top panel; green, bottom panel) and anti-b-tubulin (green, top panel), anti-Aurora B (red, bottom panel) and DAPI. Bar is 10μm.

Several enrichment protocols have been developed for the isolation and identification of proteins localized at the midbody. Thus, to confirm the presence at the midbody of HIPK2 and H2B, midbodies isolated and extracted from HeLa cells were analyzed by Western blotting (WB). Proliferating HeLa cells were enriched in elophase by nocodazole treatment, mitotic shake off, and nocodazole wash-out to release re-plated cells from prometaphase (**Figure 15**).

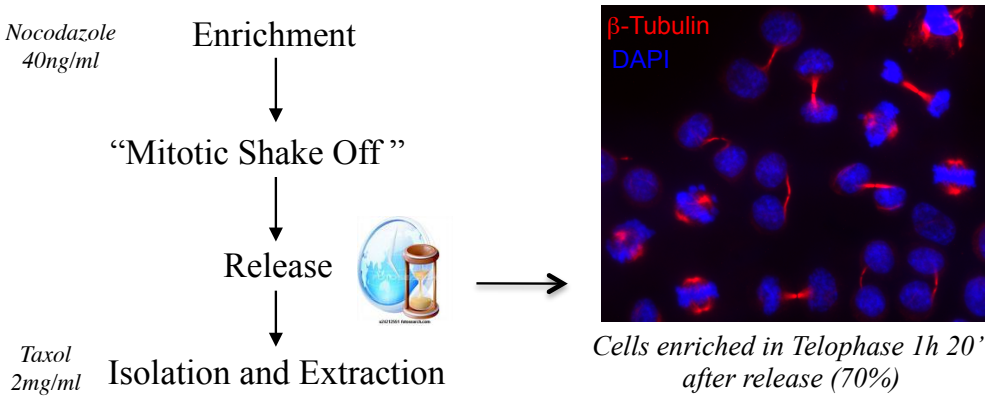


Figure 15. Representative image of an enrichment of cells at telophase (approximately 70%) from which midbodies were isolated and extracted. Cells were stained with anti-tubulin Ab (red) and DAPI.

The midbody fraction (MID) was obtained as described (Kuriyama et al., 1984) and compared by WB with equal volumes of TCEs from the same number of cells maintained in interphase (I-TCE) or enriched in telophase (T-TCE). Relative to I-TCE, both T-TCE and MID were enriched in the midbody components α-tubulin and Aurora B, while the mitochondrial protein mhsp70 and the transcription factor Sp1, used as markers of cytoplasmic and nuclear contamination, respectively, were

barely detectable in the purified MID, verifying the quality of the midbody preparations. In these conditions, HIPK2 and H2B, both total and S14P forms, were enriched in the MID, further confirming their presence in this subcellular compartment (**Figures 16**).

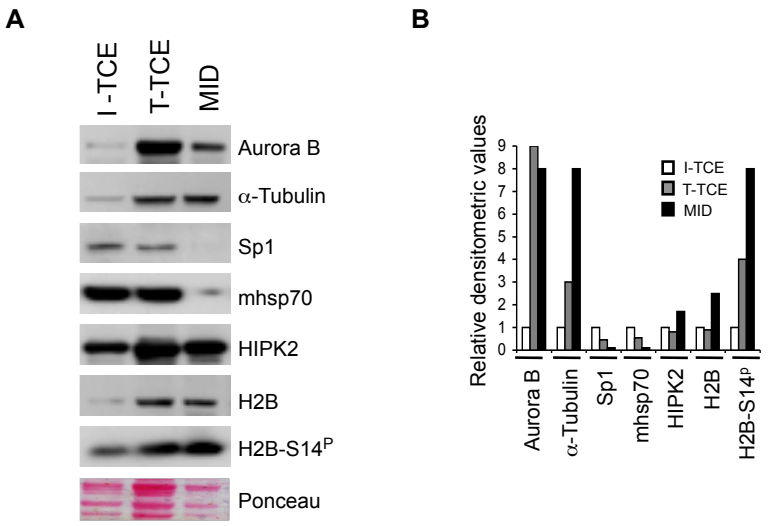


Figure 16. Localization of Endogenous HIPK2 and H2B-S14p at the Midbody

(A) HeLa culture were enriched in telophase and the midbody fraction (MID) was isolated and extracted. TCEs were derived from the same number of cells in nterphase (I-TCE) or enriched in telophase (T-TCE). A representative WB for the indicated proteins is shown. Ponceau shows the relative loading quantity. **(B)** Densitometric values were first normalized according to protein amount, then calculated taking the I-TCE level as reference value and reported in the graph.

Similar results were obtained by adopting different midbody extraction protocols (Skop et al., 2004) (data not shown). Taken together, these results show that the HIPK2/H2B interaction detected by mass-spec analysis does indeed take place at the midbody during cytokinesis.

HIPK2 Binds H2B and Phosphorylates it at S14

To determine whether HIPK2 directly interacts with H2B, in vitro binding was assayed using purified proteins. Full-length eGST-HIPK2, different deletion derivatives (**Figure 17**) and eGST alone were produced by the T7-vaccinia system, purified by glutathione-sepharose beads, and incubated with commercially available human recombinant H2B protein (**Figures 18)**.

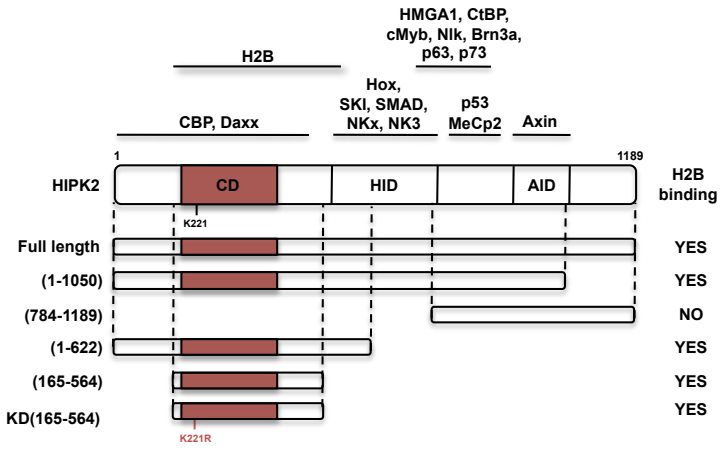


Figure 17. Schematic Representation of Murine HIPK2

The horizontal black lines on the top of the HIPK2 box indicate the known interacting regions of the indicated HIPK2 partners. Under the HIPK2 box are schematically reported the HIPK2 full length and the relative deletion mutants we constructed. On the right of each schematic protein is summarized its capacity to bind H2B. CD, catalytic domain; HID, homeobox-interacting domain; AID, auto-inhibitory domain.

eGST-HIPK2 and its C-ter deletion mutant eGST-HIPK2(1-1050) bind H2B while the N-ter deletion mutant eGST-HIPK2 (784-1189) has lost this ability, indicating that the C-ter region required for HIPK2 to bind most of its non-homeotic interactors is not relevant for interacting with H2B. A further GST pull-down

analysis performed with the sole kinase domain (aa 165-564), in the wild-type form and in the kinase defective (KD) K221R derivative, showed that this domain is sufficient for the in vitro binding of H2B, independently of the maintenance of the catalytic activity Consistent with these in vitro results, the EGFP-HIPK2 (1-622) deletion mutant expressed in HeLa cells co- immunoprecipitated with endogenous H2B. In addition, we could co- immunoprecipitate both endogenous HIPK2 and H2B from TCEs of HeLa cells with an anti-HIPK2 Ab, further supporting the notion that HIPK2/H2B complexes form in mammalian cells.

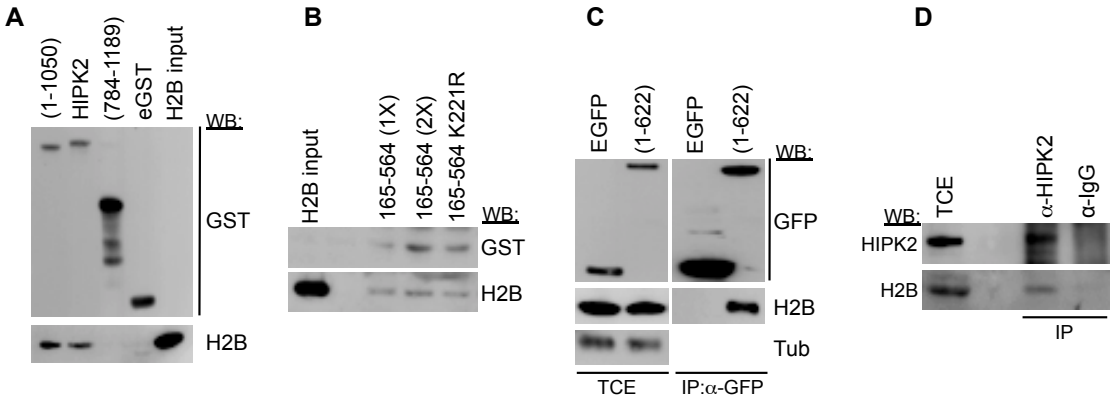


Figure 18. HIPK2 Binds and Phosphorylates H2B at S14

(A) eGST, eGST-HIPK2 and its indicated derivatives were produced by T7-vaccinia system in H1299 cells, purified by GST pull-down and incubated with human recombinant H2B. TCEs and bound complexes were analyzed by WB with the indicated Abs. **(B)** Indicated eGST-HIPK2 deletion mutants were prepared and analyzed for H2B binding in vitro as in (A). **(C)** HeLa cells were transfected with EGFP or EGFP-HIPK2 (1-622) encoding vectors. TCEs were immunoprecipitated with anti-GFP Ab and analyzed by WB with the indicated Abs. **(D)** TCE from HeLa cells was immunoprecipitated with anti-HIPK2 or anti-IgG Abs and analyzed by WB with the indicated Abs. TCE lane is loaded with 6% of the immunoprecipitated extract.

Since HIPK2 regulates several targets through its S/T kinase activity, we tested whether it can phosphorylate H2B in kinase assays in vitro. eGST-HIPK2 or its KD derivative, eGST-HIPK2-K221R, were purified and incubated with recombinant H2B in the presence of [γ32P]-ATP. As shown in **Figure 18**, wild-type HIPK2 phosphorylates H2B in this assay. HIPK2 localizes at the midbody with H2B-S14P; therefore, we asked whether HIPK2 phosphorylation of H2B occurs at this residue. A kinase assay was performed by incubating eGST-HIPK2 or eGST-HIPK2-K221R with recombinant H2B in the presence of non-radioactive ATP. WB with anti-H2B(S14) phospho-specific Ab shows that wild-type HIPK2, but not its KD derivative, phosphorylates H2B at S14, indicating that HIPK2 phosphorylates H2B at least at this site.

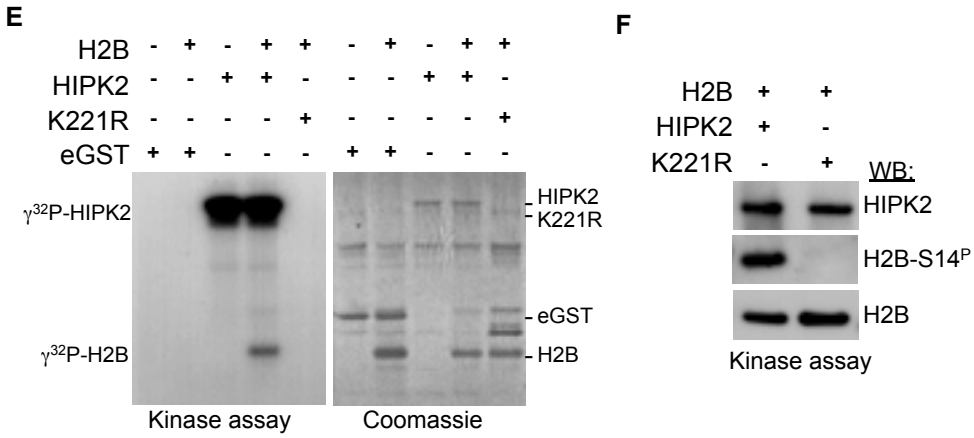


Figure 18. HIPK2 Binds and Phosphorylates H2B at S14

(E) eGST-HIPK2 and its KD derivative, eGST- HIPK2 K221R were prepared as in (A) and incubated with recombinant H2B protein in the presence of [γ32P]-ATP. Kinase reaction products were resolved by SDS-PAGE and analyzed by autoradiography (left panel) and Coomassie-blu staining (right panel). **(F)** Cold kinase assay was performed by using eGST-HIPK2 or eGST-HIPK2 K221R on recombinant H2B as in (E). Kinase reaction products were resolved by SDS-PAGE and analyzed by WB with the indicated Abs.

HIPK2 and histone H2B Localize at the Midbody Independently of the Presence of Chromosome Bridges

Different types of DNA and chromosomal dysfunctions can results in chromatin localization at the cleavage plane, the so-called chromosome bridges (Steigemann et al., 2009). Because of the role in DDR of both HIPK2 and H2B, it can be hypothesized that their midbody localization might be related to the presence of chromosome bridges. However, the frequency of HIPK2 and H2B localization we observed at the midbody (essentially 100%) would not be compatible with such an explanation, being the frequency of chromosome bridges in cytokinesis low (<10%) even in the highly aneuploid HeLa cells. Still, the presence of H2B we detected in all the midbodies was in apparent contrast with the observation made by Steigemann and coauthors, showing the H2B-mRFP autofluorescence only at midbodies with chromosomal bridges (Steigemann et al., 2009). Thus, we asked whether we could detect a tagged H2B-GFP at all the midbodies by performing IF after Ag-retrieval, as we did for endogenous HIPK2 and H2B (**Table S1**). In agreement with Steigemann's observations, in the absence of Ag-retrieval, anti-GFP immunostaining was comparable to GFP autofluorescence, being detectable in approximately 3% of the telophases, at the intercellular bridges containing chromosomal DNA, with a typical filamentous shape interconnecting the two daughter nuclei (**Figures 19A-B**). In contrast, upon Ag-retrieval, the staining was present in all the telophases analyzed, with a tubulin-like shape (**Figure 19C**).

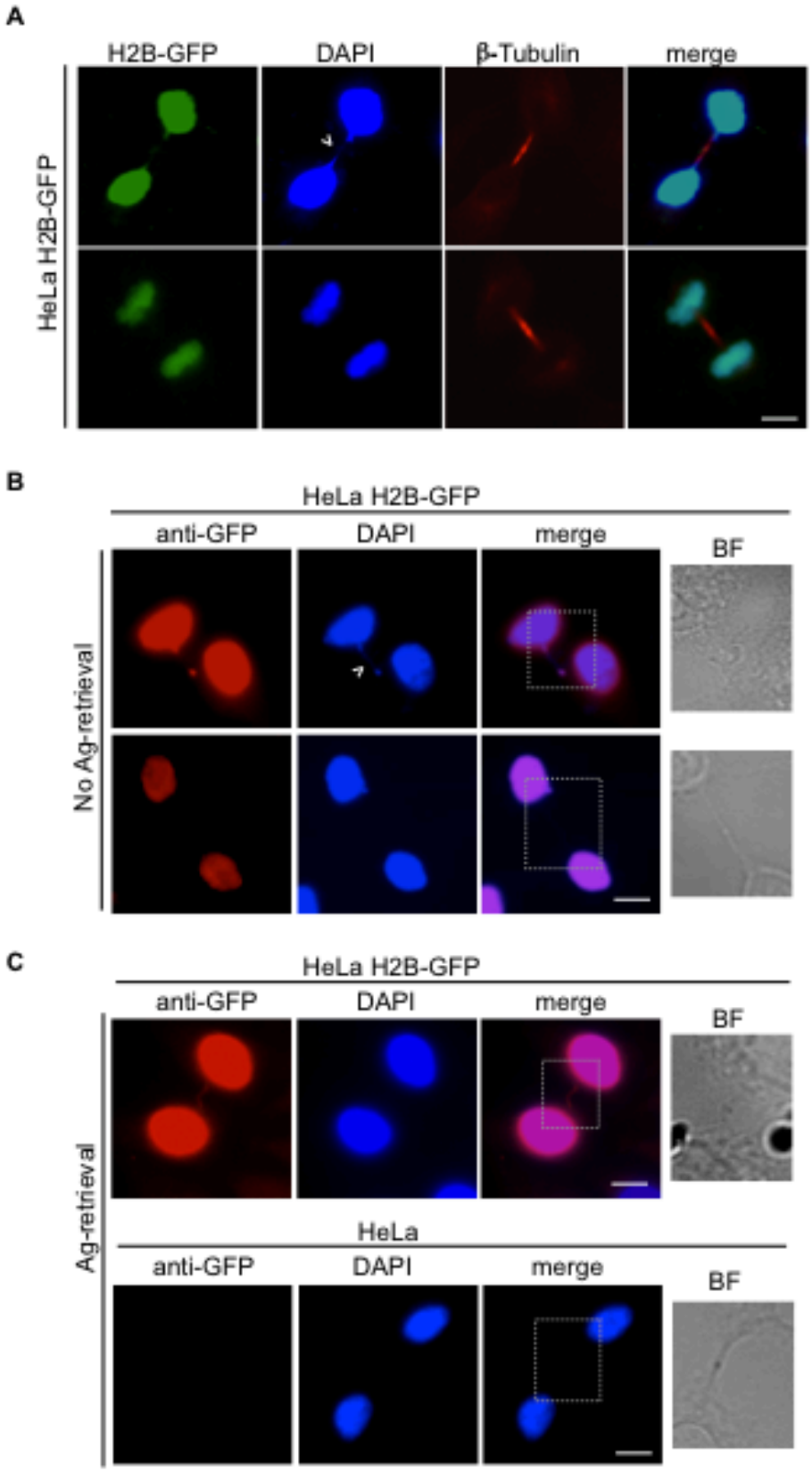


Figure 19. H2B Localizes at the Midbody Independently of the Presence of Chromosome Bridges

(A) HeLa cells stably expressing H2B-GFP were stained with anti-b-tubulin to mark midbodies and DAPI to visualize DNA. H2B-GFP was detected by autofluorescence in all the DAPI-positive bridges (@5% of the total population; n=50) (top panel, open arrowhead), while no GFP auto-fluorescence was detectable at the midbodies without chromosome bridges

(bottom panel). **(B)** HeLa H2B-GFP cells were stained with anti-GFP Ab and DAPI. In the absence of Ag-retrieval, the anti-GFP immunostaining (red) shows a H2B-GFP detection at the midbody comparable to the auto-fluorescence shown in A, *i.e.*, only in cells with chromosome bridges. Representative images of telophases with (top panel, open arrowhead) or without (bottom panel) chromosome bridges are reported. Enlargement of the midbody region (dashed-line rectangles in the merge) is reported in bright-field (BF). **(C)** H2B-GFP-expressing and parental HeLa cells were stained with anti-GFP Ab and DAPI upon Ag-retrieval. The anti-GFP immunostaining (red) shows a localization of H2B-GFP comparable to the localization of endogenous H2B (Figures 1B and 2B), *i.e.*, at all the midbodies, independently from the presence of chromosomal DNA (n=120). Representative images of a telophase without chromosome bridge are reported in the top panel. No staining with anti-GFP was observed in parental, untrasfected HeLa cells (representative images are reported in the bottom panel).

These results indicate that H2B-GFP, like the endogenous H2B, does localize at the midbody even in the absence of chromosomal DNA. Similar results were obtained with H2B in frame with different tags (data not shown). In agreement with these results, we found the phosphorylated form H2B-S14P at all the midbodies, but not in the nucleosomal DNA of chromosome bridges (data not shown), supporting the existence of two different H2B functions. Overall, these results strongly indicate that HIPK2 and H2B can co-localize with the midbody components, independently of the presence of chromosomal DNA.

HIPK2 is Required for Faithful Cytokinesis

The results obtained thus far suggest that the midbody localization of HIPK2 and H2B is not related to their DDR activities or the presence of nucleosomal DNA. Therefore, we investigated whether these two proteins might have a direct role in cytokinesis by loss-of-function experiments. HIPK2 depletion by RNAi (HIPK2i) was obtained in HeLa cells by transduction of three HIPK2-specific stealth-RNA sequences employed together or separately with comparable results, while control depletion (Ctri) was obtained by universal negative control sequences. Starting at day 5 post-transfection, asynchronous HIPK2i and Ctri HeLa cells were analyzed by time-lapse live-cell imaging. A large fraction of the HIPK2i cells that underwent division during the 24 hour imaging session became binucleated, whereas Ctri cells divided normally and originated mononucleated daughter cells. After an average of 1,5 hours from metaphase chromosome alignment, cells in the control cultures divided into two daughters that decondensed DNA and re-established adhesion to the dish, whereas in a time-frame of 3 to 6 hours, 20% (n=53) of the HIPK2i dividing cells formed midbodies but failed abscission and the daughter cells collapsed back into binucleated cells. IF analysis of parallel cultures showed a strong induction in the number of binucleated cells (30±5% vs 5±1%) and of syncytium-like structures (37±1% vs <1%), again indicating cytokinesis failure (**Figures 20** and **Movies S1A and S1B**).

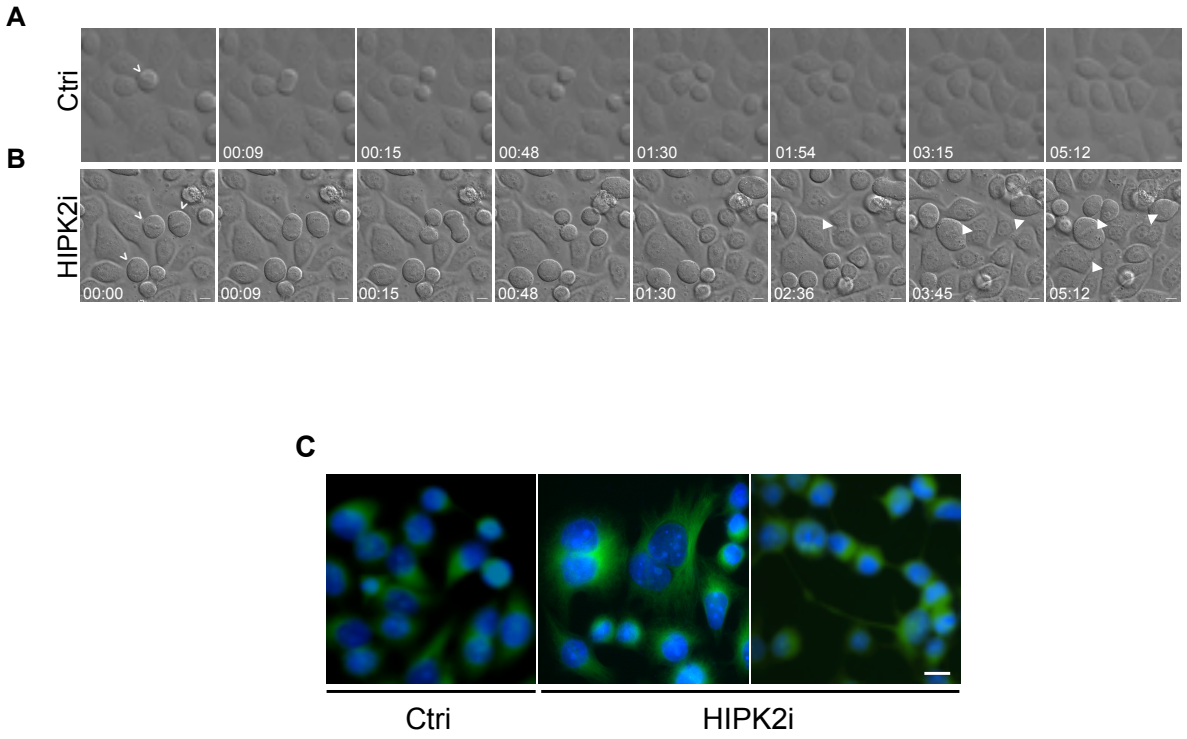


Figure 20. HIPK2 Depletion is Associated with Cytokinesis Failures

Control (Ctri) and HIPK2 depleted (HIPK2i) HeLa cells (transfection efficiency @80%) were employed as total populations. Stills from time-lapse recording of HeLa Ctri **(A-movie S1A)** and HIPK2i **(B-movie S1B)** cells 5 days post-transfection are shown. Ctri cells divided and remained mono-nucleated while HIPK2i cells became bi-nucleated after failing abscission. Open arrowheads indicate the cells to follow; close arrowheads indicate the end-up into binucleated cells. **(C)** Representative fields of Ctri and HIPK2i HeLa cells stained with anti-tubulin Ab (green) and DAPI. The presence of bi-nucleated cells (middle panel) and syncytium-like structures (right panel) is detectable in the HIPK2i cells compared to the Ctri (left panel)

Next, we evaluated whether similar cytokinesis defects can be observed in non-tumor, primary Hipk2 knockout cells. Mouse embryo fibroblasts (MEFs) from littermate Hipk2+/+ and Hipk2-/- embryos were maintained in culture for a few passages and subjected to microscopic analysis at different time after plating. Starting from passage 3, we observed a time-dependent accumulation of bi- and

multinucleated cells in Hipk2-/- MEFs compared to their Hipk2+/+ counterparts. This phenotype was associated with a strong appearance of a high percentage of dividing cells that remained interconnected by LIBs. Comparable results were obtained in HIPK2 depleted human fibroblasts (**Figure 21**).

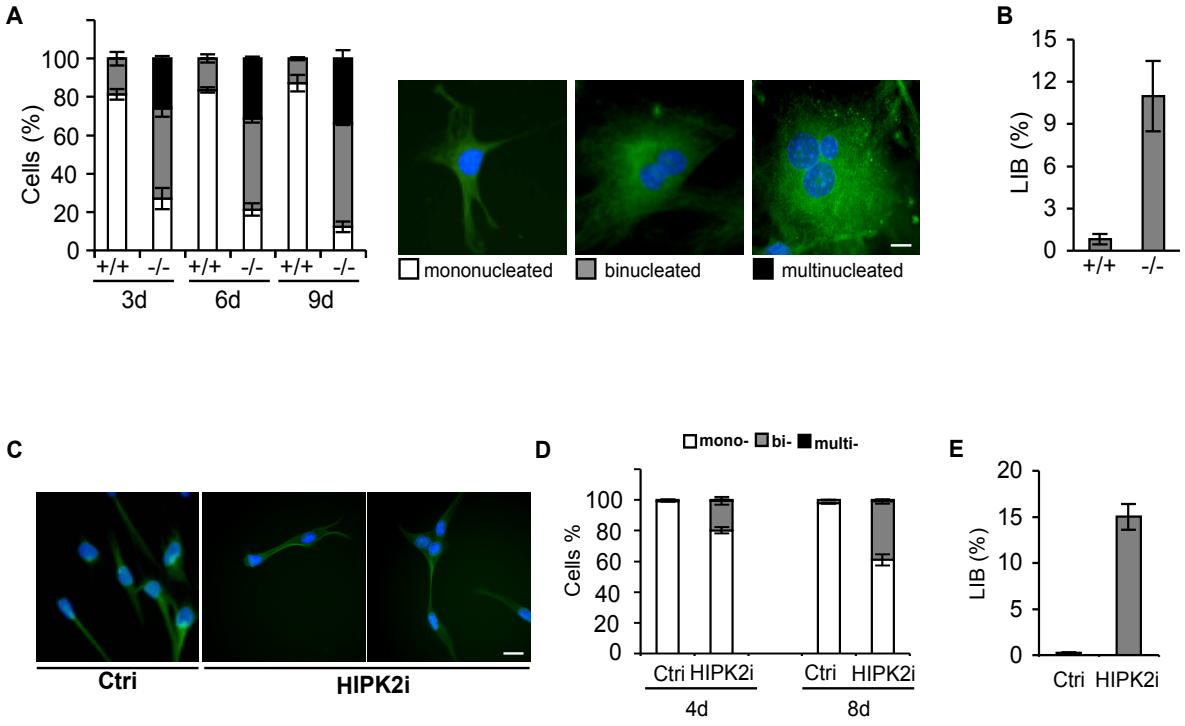


Figure 21. HIPK2 Depletion is Associated with Cytokinesis Failures

(A) MEFs from littermate *Hipk2*+/+ and *Hipk2*-/- embryos were stained, at the indicated days (d) after plating, with DAPI and anti-tubulin Ab (green) to identify the cytoplasms in interphase and the midbodies or the LIBs in telophase. The percentage (left panel) and the morphology (right panel) of mono-, bi- and multi- nucleated cells is reported. About 1,000 cells per sample were scored for the presence of one, two or more nuclei/cell and the data are represented as mean ± SD. **(B)** Percentage of LIBs in MEFs from four different *Hipk2*+/+ and *Hipk2*-/- mice. About 3,000 cells per sample were scored and the data are represented as mean ± SD. **(C)** Representative images of cell morphology of Ctri and HIPK2i HFs 6 days after transfection. Cells were stained with anti-tubulin Ab (green) and DAPI. Bar is 10µm. **(D-E)** HFs were stained, at the indicated days after transfection, with anti-tubulin Ab and DAPI. About 1,000 cells per sample were scored for the presence of one, two or more nuclei/cell (D) and the cells with LIBs (E).

Of relevance, re-expression of HIPK2 in the Hipk2-/- MEFs abolished all the observed defects by reducing the number of bi- and multi- nucleated cells and suppressing the formation of LIBs (**Figure 22**).

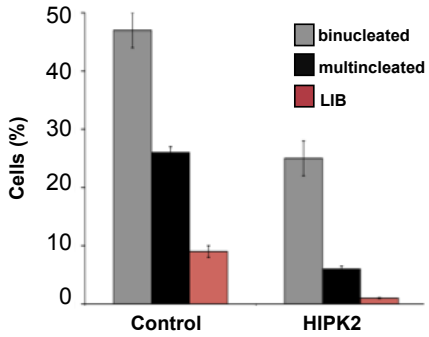


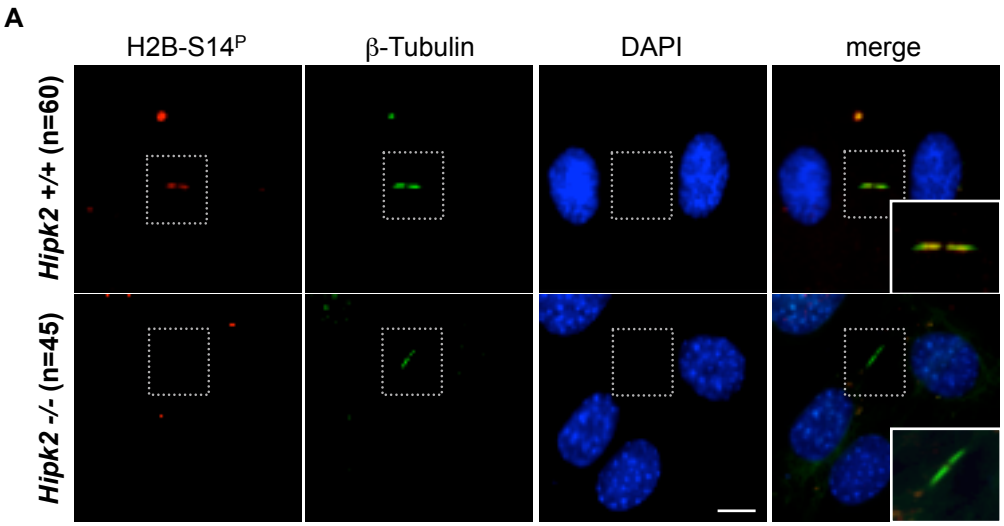
Figure 22. HIPK2 Depletion is Associated with Cytokinesis Failures

Reconstitution of wild-type HIPK2 expression in *Hipk2*-/- MEFs abolishes the cytokinetic defects. *Hipk2*-/- MEFs were transfected with control vector (Ctr) or EGFP- HIPK2 expressing vector (HIPK2). Cells were stained and analyzed 60hrs post- transfection for the percentages of mono-, bi- and multi-nucleated cells and the percentages of LIB. Only EGFP-positive cells were scored. Data are represented as mean ± SD.

Altogether, these data show that HIPK2 depletion by RNAi or targeted gene disruption impairs abscission and induces accumulation of cytokinesis-dependent aberrations.

HIPK2 is Required for H2B-S14 Phosphorylation at the Midbody

Cytokinesis failures might be due to furrow regression induced by problems in chromosome disjunction or the presence of chromosomal bridges on the cleavage plane (Steigemann et al., 2009). We did not observe any significant differences between the HIPK2 proficient and deficient cells in i) the segregation of chromatin in two equal masses without evidence of lagging or unaligned chromosomes, ii) the presence of chromatin bridges, iii) the amount of spontaneous g-H2Ax positive DSBs (data not shown), suggesting that the cytokinesis failure we observed in the HIPK2- defective cells is not secondary to DNA or chromosome abnormalities induced by HIPK2 inactivation. Thus, we asked whether HIPK2 inactivation impairs H2B localization and/or S14 phosphorylation at the midbody. Midbody localization of H2B was assessed in Hipk2+/+ and Hipk2-/- MEFs by IF with anti-H2B and anti-H2B(S14) phospho-specific Abs. As shown in **Figure 23** , H2B, but not its S14P form, is detectable at the midbodies of Hipk2-/- MEFs, indicating that H2B localizes at midbody independently of HIPK2, whereas its phosphorylation at S14 requires the kinase.



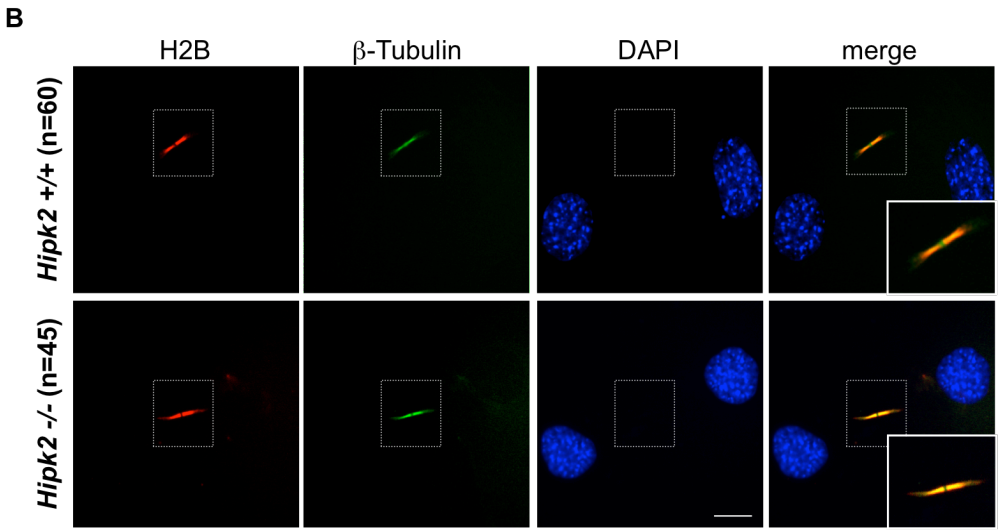


Figure 23. HIPK2 Knockout Impairs H2B-S14P but does not Affect H2B Localization at the Midbody

(A) H2B phosphorylation at S14 requires the presence of HIPK2. MEFs were stained with anti-p-Histone H2B-S14[(1)] Ab (red), anti-tubulin Ab (green) and DAPI. H2B-S14P is detectable at midbody in *Hipk2*+/+ MEFs (top panels), but not in *Hipk2*-/- MEFs (bottom panels). **(B)** H2B localizes at midbody independently of HIPK2. MEFs were stained with anti-H2B[(2)] Ab (red), that preferentially recognize extra-nucleosomal H2B, anti-tubulin Ab (green) and DAPI. H2B is detectable at midbody in both *Hipk2*+/+ (top panels) and *Hipk2*-/- (bottom panels) MEFs.

HIPK2-mediated H2B-S14 Phosphorylation is Required for Cytokinesis

Since the absence of HIPK2 impairs H2B-S14P, we asked whether this event is crucial for the completion of cytokinesis. We expressed the KD HIPK2-K221R mutant in Hipk2-/- MEFs and showed that, at variance with wild-type HIPK2, the KD mutant is not able to abolish the defects associated with cytokinesis failure (**Figure 24**), confirming the requirement for the HIPK2 catalytic activity for the completion of cell division.

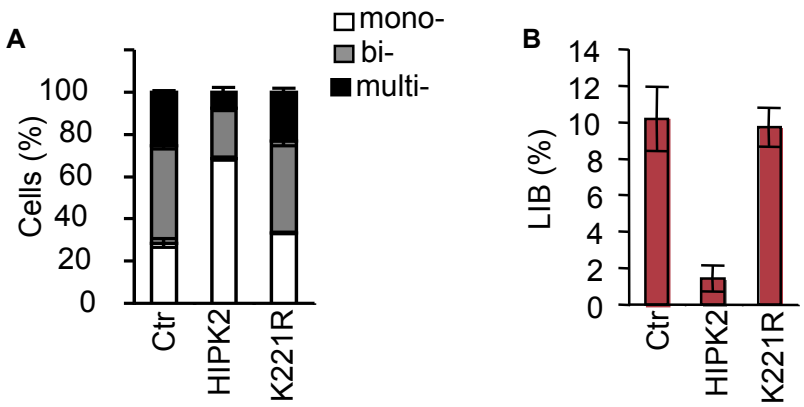


Figure 24. H2B-S14 Phosphorylation by HIPK2 is Required for Cytokinesis: The KD HIPK2-K221R mutant fails to abolish the cytokinetic defects of Hipk2-/- MEFs. Hipk2-/- MEFs were transfected with control, EGFP vector (Ctr), EGFP-HIPK2 (HIPK2) or EGFP-HIPK2-K221R (K221R) expressing vectors. At 48 hrs post- transfection, cells were stained with anti-b-tubulin Ab and DAPI; about 3,000 EGFP- positive cell per sample were scored for the percentages of mono-, bi- and multinucleated cells **(A)** and LIBs **(B)**. Data are represented as mean ± SD.

Next, we evaluated whether expression of a phospho-mimetic H2B-S14D derivative, in which the S14 residue was replaced with an aspartic acid to mimic constitutive phosphorylation, is able to overcome the requirement for HIPK2 in cytokinesis. To this aim, Hipk2-/- MEFs were transduced with GFP-tagged wild-type H2B, H2B-S14D, and a non-phosphorylatable H2B-S14A derivative. Both H2B and H2B-S14A have no effects on the cytokinesis defects that accumulate in the Hipk2-/- MEFs, whereas H2B-S14D abolished all the observed defects and rescued the normal phenotype (**Figure 25**) like wild-type HIPK2.

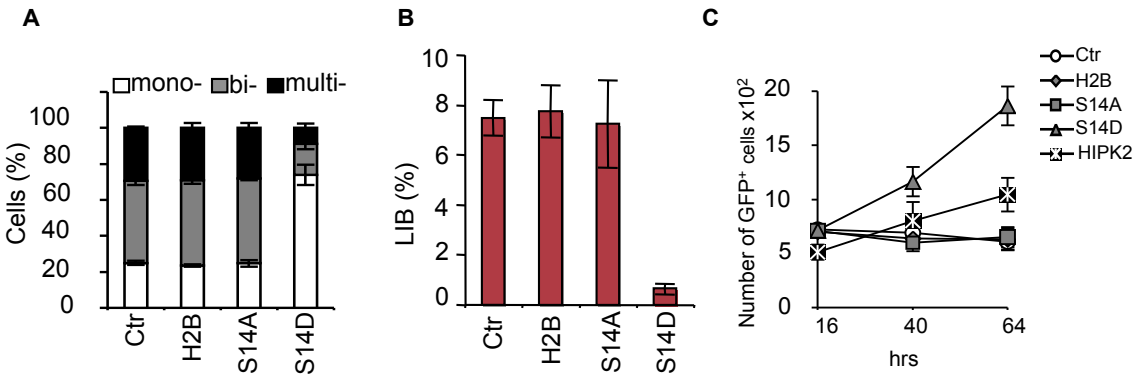


Figure 23. H2B-S14 Phosphorylation by HIPK2 is Required for Cytokinesis: Expression of a phospho-mimetic H2B-S14D in Hipk2-/- MEFs abolishes the cytokinetic defects and restores proliferation. Hipk2-/- MEFs were transfected with control vector (Ctr) or expression vectors encoding GFP-tagged wild-type H2B (H2B), unphosphorylatable H2B-S14A (S14A) and phospho-mimetic H2B-S14D (S14D). Three days post-transfection GFP-positive cells were stained and analyzed as above for the percentages of mono-, bi- and multinucleated cells **(A)** and LIBs **(B**). Data are represented as mean ± SD. **(C)** Hipk2-/- MEFs were transfected with the vector described above plus a EGFP-HIPK2 carrying vector. Starting at 16 hrs post- transfection, the numbers of GFP-positive cells were measured by direct counting of each dish and the data of three different experiments are represented as mean ± SD.

Strikingly, the sole H2B-S14D expression was able to restore proliferation of the Hipk2-/- MEFs, supporting a key role for H2B-S14 phosphorylation in the complete execution of cytokinesis.

DISCUSSION

Our study reveals an unexpected subcellular localization and biological function of HIPK2 and histone H2B in cytokinesis. We show that a catalytically active HIPK2 is required for faithful cytokinesis through the phosphorylation of histone H2B at S14. This phosphorylation allows the completion of abscission, as demonstrated by the cytokinetic failure of HIPK2-defective cells and by the restoration of their normal phenotype through the sole expression of a phospho-mimetic H2B-S14D histone. In particular, HIPK2-defective cells show different signs of cytokinesis failure and the accumulation of tetra- and polyploid cells. These data uncover a role for HIPK2 in the prevention of tetraploid cell formation, a function that might contribute to the HIPK2 tumor suppressing activity, and reveal a DDR-independent, extra-chromosomal function of histone H2B-S14P.

A DDR-Independent Interaction of HIPK2 and H2B

We employed several human and mouse cells, including tumor (HeLa, HEK293, MCF7), immortal (C2C12, HF, AHH1, MEF), and primary cells (Hipk2+/+ and Hipk2-/- MEFs), different tagged-HIPK2 proteins, and a series of Abs (Table S1) to confirm the localization of HIPK2 and H2B at the midbody and to assess whether their presence was independent of chromosome bridges. In fact, the completion of cytokinesis by abscission needs to await complete clearance of chromatin from the cleavage plane. Several defects such as dysfunctional telomeres, DNA DSBs,

misregulated chromosome segregation, cohesion, or decatenation can result in the persistance of chromosomal bridges that are visualized by the presence of nucleosomal histones (Steigemann et al., 2009 and references therein). Interestingly, we found histone H2B at the spontaneous chromosome bridges of HeLa cells, but it was not phosphorylated at S14 and was not immuno-stained for HIPK2. In contrast, all the apparently normal telophases have both H2B-S14P and HIPK2 colocalized with midbody markers, indicating an extra-chromosomal function for the modified histone. This conclusion is further supported by the detection of H2B-GFP, whose autofluorescence is visible only on chromosomal bridges, at all the midbodies upon Ag-retrieval and IF with anti-GFP Ab. Problems of Ab penetration for Ag-recognition of midbody components have been reported and Ag-retrieval, commonly performed in immunohistochemistry, may allow the removal of soluble proteins that mask the Ag and reveal epitopes hidden in complex structures (Saxton and Mcintosh, 1987). Since with Ag-retrieval and anti-GFP Ab we detect an H2B localization that, at variance with autofluorescence, completely overlaps the endogenous H2B, it is plausible that the autofluorescent tag is masked by other midbody components. This observation calls attention to the limits that autofluorescent tagged-proteins might present, despite their great value in live-cell imaging.

An Extra-Chromosomal Activity of H2B

Histones are assembled in the nucleosome as core (H2A, H2B, H3 and H4) and linker (H1) histones. In mitosis, a few site-specific phosphorylations of both linker

and core histones are evolutionarily conserved and contribute to chromatin condensation and sister chromatid segregation (Cheung et al., 2000). Phosphorylation of histone H2B at S14 in human and S10 in yeast has been linked to DDR and chromatin condensation in apoptosis and meiosis (Cheung et al., 2003; Ahn et al., 2005a and 2005b). All these conditions are associated with chromatin remodeling. In contrast, here we observe a cytokinesis-specific localization of H2B and its phosphorylation at S14, independent of the presence of chromosomal DNA, DDR, and/or apoptosis. Interestingly, histone exchange and deposition kinetic studies revealed that H2B is the most rapidly and abundantly exchanged core histone (Kimura and Cook, 2001) and, recently, extra-chromosomal H2B was shown to be involved in the antiviral innate immune responses (Kobiyama et al., 2009). A few other extra-chromosomal locations and activities of histones have been observed. In apoptotic conditions, histone H1.2 is discharged from the nucleus into the cytoplasm and induces cytocrome C release (Konishi et al., 2003). Phosphorylated histone H1 has also been found in the cytoplasm of M phase HeLa cells (Bleher and Martin, 1999), while H3- S10P has been shown to co-stain with Aurora B in mitosis and cytokinesis (Song et al., 2007); however, the function of this extra-chromosomal distribution is unknown. In addition, histones are under surveillance by an increasing list of chaperones involved in many aspects of histone metabolism, including transport, storage, and post-translational modifications (Loyola and Almouzni, 2004). Thus, it is reasonable to hypothesize that, besides nucleosome-remodeling activities, chaperones direct histones to extra-chromosomal locations and functions. Confinement to specific sub- cellular localizations, like the

midbody, might explain why a pro-apoptotic modification such as H2B-S14P can contribute to cytokinesis without promoting apoptosis. It was reported that expression of a phospho-mimetic H2B-S10E mutant in S. cerevisiae induces chromatin condensation and cell death (Ahn et al., 2005a), while we did not find any evidence of apoptosis in our Hipk2-/- MEFs upon transfection of the phospho-mimetic H2B-S14D mutant. The absence of apoptosis is not a specific feature of these cells, in which H2B-S14D expression rescued the cytokinetic defects, since it also did not elicit apoptosis in the HIPK2-proficient HeLa cells (data not shown). It is possible that we did not observe apoptosis because the p53 pathway is impaired in our mammalian cells; however, whether due to cell-specific resistance or to phylogenetic distance, the absence of apoptosis allowed us to highlight the H2B cytokinetic function. Because of the possible implication of the p53 pathway in modulating the functional consequences of the HIPK2-H2B defects (see below), it will be interesting to discriminate between these two possible explanations. At this point, what is the activity of H2B-S14P at the midbody can only be a matter of speculation. Upon phosphorylation, H2B tails develop an intrinsic “aggregation” property that might mediate chromatin compaction in “cis” and protein recruitment in “trans” (Ahn et al., 2005a). By analogy to what has been proposed for chromatin, in cytokinesis this aggregation property might contribute to intercellular bridge constriction in “cis” and recruit regulatory and effector components in “trans”.

HIPK2 in the Control of Cytokinesis

We observed different signs of cytokinesis failure in HIPK2-depleted and -defective cells, such as time-dependent accumulation of LIBs and syncytium-like cells, reduction in the number of cells at the midbody stage, regression of the cleavage furrow, and accumulation of tetra and polyploid cells. These signs are usually observed in cells with impaired abscission (Normand and King, 2010; Steigenmann and Gerlich, 2009), supporting a role for HIPK2 and its target H2B in this stage of cell division. A large number of molecular factors have been identified as critical components of the abscission machinery, though their aggregated functions are still poorly understood (Guizzetti and Gerlich, 2010). In addition, due to the dependency of each step of cytokinesis on the proper execution of the prior stage, it is not always easy to discriminate among roles played in the different steps. Indeed, we could observe HIPK2 and H2B, but not in its S14P form, at the central spindle, in anaphase; however, the findings that H2B can reach the midbody independently of HIPK2 and that a phospho-mimetic H2B-S14D mutant is sufficient to rescue all the cytokinesis defects present in the Hipk2-/- MEFs indicate that these defects are not due to other types of HIPK2-mediated functions, such as regulation of gene expression, and strongly support a direct involvement of HIPK2 in abscission.

Although Hipk2-/- mice can survive and be fertile (Isono et al., 2006), they are significantly smaller than their wild-type littermates throughout adulthood (Trapasso et al., 2009), they are born at a reduced mendelian rate (G.M.P. and A.F., unpublished data), and proliferation defects have been observed in sensory neurons (Wiggins et al., 2004) and in MEFs (Trapasso et al., 2009). Of relevance,

Hipk1/Hipk2 double knockout embryos die between 9.5 and 12.5 days post-coitus with cell proliferation defects (Isono et al., 2006), indicating redundancy at least between the HIPK1 and HIPK2 members of the HIPK family. Interestingly, we observed extremely rare events of spontaneous immortalization in our Hipk2-/- MEFs. The immortalized clones display HIPK2-independent H2B-S14P at the midbody (C.R. and S.S., unpublished data), indicating the existence of an in vitro selection for rescue mechanism(s) and strongly supporting the relevance of H2B-S14P in cell division. It will be interesting to verify whether this rescue is induced by other HIPKs, by DYRKs, that have striking homology with HIPKs and were shown to phosphorylate H2B in vitro (Becker et al., 1998), or by other kinases known to phosphorylate H2B- S14 during DDR and apoptosis, such as Mst1 and PKCd (Cheung et al., 2003; Mecklenbrauker et al., 2004).

HIPK2 as a Tumor Suppressor

The oncosuppressing functions of HIPK2 has been thus far thought to reside in its mechanistic link with the p53 tumor suppressor and the pro-apoptotic activities of the kinase in response to different types of stress in p53-dependent and -independent manners. Indeed, resistance to spontaneous and induced apoptosis has been described in cell and mouse models, and in human cancers. The present study shows that HIPK2 depletion induces cytokinesis failure and accumulation of tetraploid and polyploid cells, a genetically unstable state that can lead to aneuploidy and ultimately to cancer (Ganem et al., 2007), suggesting that HIPK2 inactivation might contribute to tumorigenesis also by generating tetraploidy.

Although the existence of a p53-dependent "tetraploid checkpoint" was not confirmed (Uetake and Sluder, 2004; Aylon and Oren, 2011), tetraploid cells arising from cytokinesis failure have been shown to activate p53 and undergo apoptosis (Castedo et al., 2006) or be prone to neoplastic transformation in a p53-null context (Fujiwara et al., 2005). Because of the key role of HIPK2 in the pro-apoptotic activity of p53, we hypothesize that HIPK2 inactivation may at once generate tetraploids and suppress their safety control.

Table S1. Antibodies and Heat-Induced Ag-Retrieval Techniques Employed for IF

Antibody	Manufacturer	Dilution	Species	Ag-retrieval§
Aurora B (AIM-1)	BD Biosciences	1:100	Mouse	None
FLAG	Sigma	1:100	Rabbit	None
GFP	Santa Cruz Biotech.	1:100	Mouse	Citrate Buffer pH 8.9, 25', 80°C
HA	Roche	1:2000	Mouse	None
HIPK2(1)	Iacovelli et al., 2009	1:100	Mouse	Citrate Buffer pH 6, 45', 96°C
HIPK2(2)	Pierantoni et al., 2007	1:100	Rabbit	None
Histone H2B(1) *	Millipore	1:100	Rabbit	Citrate Buffer pH 8.9, 25', 80°C
Histone H2B(2) **	Cell Signalling	1:100	Rabbit	None
Histone H2B(3) ***	Gift from Dr. Monestier	1:100	Mouse	Diva Decloaker sol. 30', 125°C
p-Histone H2A.X-S139	Millipore	1:100	Rabbit	None
p-Histone H2B-S14(1)	Santa Cruz Biotech.	1:100	Rabbit	None
p-Histone H2B-S14(2)	Millipore	1:100	Rabbit	None
β-Tubulin-FITC	Sigma	1:500	Mouse	None
β-Tubulin-Cy3	Sigma	1:500	Mouse	None

§Heat-induced Ag-retrieval was performed by employing Novocastra TM-Epitope Retrieval Solutions (Leica) at the indicated temperatures, or Diva Decloacker solution (Biocare medical) by using a Pascal's digital electric pressure cooker (DakoCytomation).

*Anti-H2B(1) was produced by immunization with a synthetic peptide corresponding to the carbossi-terminus (residues 118-126) of human H2B.

**Anti-H2B(2) was raised against the amino-terminus of histone H2B; by IF it recognizes preferentially the extra-chromosomal H2B.

***Anti-H2B(3) (Ab LG2-2), kindly provided by M. Monestier, recognizes the amino-terminus of H2B (residues 1-13) as described (Monestier et al., 1993).

EXPERIMENTAL PROCEDURES

- **Cells, Culture Conditions, and Vaccinia Virus Infection**

HeLa, C2C12, H1299, HEK293, and hTert-immortalized HF (Lazzari et al., 2011) were cultured in DMEM supplemented with 10% heat-inactivated fetal bovine serum (FBS, Invitrogen). MEFs were explanted at 14.5 days post coitus and cultured in DMEM with high-glucose, supplemented with 20% heat-inactivated FBS (HyClone, Thermo Scientific). For DNA damage, subconfluent cells were g-irradiated (5Gy/dish) by an IBL 437C Irradiator (CIS bio international). For live cell imaging, HeLa cells were cultured in DMEM medium without phenol red, supplemented with 10% heat- inactivated FBS (Invitrogen). Recombinant vaccinia virus vTF7-3 carrying the bacteriophage T7 gene 1, kindly provided by Dr. B. Moss, was propagated in HEK293 cells and used by standard techniques (Fuerst et al., 1986).

- **GST Pull-down, Electroforesis, and Mass Spectrometry**

To obtain high levels of eGST or eGST-HIPK2 fusion protein in human cells, H1299 cells were infected with vTF7-3 followed by transfection with pcDNA3-eGST or pcDNA3-eGST-HIPK2 plasmids using Lipofectamine (Invitrogen) as described (Cecchinelli et al., 2006). TCEs of transduced H1299 cells were prepared 16h post- transfection by lysis buffer [50mM Tris-HCl (pH 7.4), 600mM NaCl,

5mM EDTA (pH 8.0), 1mM DTT, 0.5% NP-40]. After GST pull-down, eGST and eGST-HIPK2 bound proteins were resolved onto NuPAGEÒ Novex Bis-Tris Gels (Invitrogen) and stained with Colloidal Blue Staining Kit (Invitrogen) following manufacturer's instructions. Interesting bands were cut and processed in-gel via tryptic proteolysis. Each peptide mixture was analyzed by MALDI-ToF STR (Applied Biosystems) mass spectrometer. The protein identifications, from resulting peptide mass fingerprint (PMF), were achieved by Mascot search engine.

- **Expression Vectors and Transfection**

The following plasmids were employed: FLAG-HIPK2, pEGFP-HIPK2, pEGFP-HIPK2-K221R and pEGFP-HIPK2 deletion mutants (Rinaldo et al., 2007b); pcDNA3GST, pcDNA3GST-HIPK2 and pcDNA3GST-HIPK2-K221R (Cecchinelli et al., 2006), pBOS-H2B-GFP (BD-Pharmingen). H2B-S14A-GFP and H2B-S14D-GFP mutants were constructed by the QuickChange site-directed mutagenesis kit (Stratagene). To construct the pcDNA3-GST-HIPK2 deletion mutants and pEGFP-HIPK2(1-622), DNA fragments of the murine Hipk2 gene were amplified from pBKS clone 46 (D'Orazi et al., 2002) by PCR with Pfu DNA polymerase in the presence of specific primers. All the constructs were analysed by sequencing. The expression vectors were transfected by using Lipofectamine LTX and Plus reagent (Invitrogen), according to manufacturer's instructions.

- **Immunofluorescence Microscopy**

For immunofluorescence experiments, cells were seeded onto poly-L-lysine coated coverslips. Cells were fixed in ice-cold methanol or 2% formaldehyde, washed three times in phosphate buffered saline (PBS), permeabilized in 0.25% Triton X-100 in PBS for 10 min., and then blocked in 0.2% Triton X-100, 5% bovine serum albumin (BSA) in PBS for 60 min. before the required primary Abs were applied. To reduce non-specific hydrophobic interactions, primary Abs were incubated in the presence of non-ionic detergent (0.2% Triton X-100, 5% BSA in PBS). Appropriate secondary FITC- or TRITC-conjugated Abs (Jackson Immuno Research Lab) were used. When required, heat-induced Ag-retrieval was peformed after permeabilization. Table S1 shows a detailed list of the Abs and heat-induced Ag-retrieval techniques employed. Fluorescence signals were recorded by using a Leica DMIRE2 microscope equipped with a Leica DFC 350FX camera and elaborated by a Leica FW4000 deconvolution software (Leica).

- **Western Blot, Immunoprecipitation, and Kinase Assay**

For Western Blotting, TCEs were prepared in RIPA buffer [50mM Tris-HCl (pH 8), 600mM NaCl, 0.5% sodium deoxycholate, 0.1% SDS, 1% NP40 and 1mM EDTA] supplemented with protease-inhibitor mix (Roche). For co-immunoprecipitations, TCEs were prepared in non-denaturing lysis buffer (NDLB) [50mM Tris-HCl (pH 7.5), 150mM NaCl, 0.5% Triton-X100, 1mM EDTA]. The following Abs were employed: rabbit anti-HIPK2 (kindly provided by L. Schmitz), anti-alpha-tubulin

moAb (Immunological Sciences), anti-Aurora B (AIM-1) moAb (BD Biosciences), anti- mHsp70 moAb JG1 (Affinity Bioreagent), rabbit anti-Sp1 polyclonal Ab PEP2 and anti-GFP moAb (Santa Cruz Biotechnologies), anti-H2B moAb (LG2-2, kindly provided by M. Monestier) (Monestier et al., 1993), rabbit anti-H2B polyclonal Ab and rabbit anti-phosho H2B (S14) polyclonal Ab (Millipore), anti-GST moAb (kindly provided by M. Fanciulli), rabbit-anti mouse IgG, HRP-conjugated goat anti-mouse and anti-rabbit (Cappel). Immunoreactivity was determined using the ECL-chemioluminescence reaction (Amersham Corp) following the manufacturer's instructions. Kinase assays were performed as reported (Lazzari et al., 2011).

- **Midbody Isolation and Extraction**

HeLa cells were enriched in telophase by treatment with nocodazole (40ng/ml for 3 hours) followed by mitotic shake off, nocodazole wash-out, and incubation of the collected cells for about 80 min. to reach telophase stage. Midbodies were isolated as described by Kuriyama (Kuriyama et al., 1984) and extracted using an extraction buffer [50mM Tris-HCl (pH 7.4), 600mM NaCl, 0.1% SDS, 0.5% NP40, 1mM DTT, 5mM EDTA] supplemented with protease-inhibitor mix and phosphatase inhibitor mix (Roche). TCEs from unsynchronized Interphase and Telophase-enriched cells were obtained in the same manner and analyzed by WB together with midbody's extracts.

- **GST Pull-Down and in Vitro Binding Assay**

For in vitro binding experiments, eGST-HIPK2 fusion protein and its derivatives were expressed in H1299 cells as described above, and purified directly from TCEs using Glutathione-Sepharose 4 Fast Flow (GE Healthcare). In particular, TCEs were prepared in NDLB supplemented with protease-inhibitor mix (Roche) and GST-tagged proteins were incubated for 2hrs at 4°C with glutathione sepharose beads. Pull-down GST-tagged proteins were washed three times with NDLB and incubated with 500 ng of recombinant human H2B (Upstate) in binding buffer [50mM Tris-HCl (pH 7.5), 200mM NaCl, 0.5% Triton-X100 and 1mM EDTA]. Bound H2B was analyzed by WB.

- **RNA Interference, RNA Extraction, and Quantitative Real-time RT-PCR**

RNA interference was obtained by HIPK2-specific (HIPK2i) stealth RNAi sequences (a mix of three different sequences employed alone or in combination with similar readout) and by universal negative control stealth RNAi Negative Medium GC Duplexes (Invitrogen). Cells were transduced with 40nM of siRNA using RNAiMAX reagent (Invitrogen) according to the manufacturer's instructions. Red fluorescent oligonucleotides (Block-it, Invitrogen) were used to evaluate transfection efficiency. In extraction and Real-time RT-PCR were performed as described (Lazzari et al., 2011).

- **Live Cell Imaging**

Cells seeded in 35 mm dishes (81156, ibiTreat, Ibidi) and transfected as described above were observed under an Eclipse Ti inverted microscope (Nikon) using a Plan Apo 60x 1.4 NA oil immersion objective (Nikon). During the whole observation, cells were kept in a microscope stage incubator (Basic WJ, Okolab), at 37°C and 5% CO2. DIC images were acquired every 3 minutes over a 24hrs period by using a DS-Qi1Mc camera and the NIS-Elements AR 3.22 software (Nikon). Image and video processing were performed with NIS-Elements AR 3.22.

- **Statistical Analysis**

The experiments have been repeated from three to five times and the results obtained are presented as means ± SD. Significant changes were assessed by using Student's t-test for unpaired data, and P-values < 0.05 were considered significant.

REFERENCES

Ahn, S.H., Cheung, W.L., Hsu, J.Y., Diaz, R.L., Smith M.M., Allis, C.D. (2005a). Sterile 20 kinase phosphorylates histone H2B at serine 10 during hydrogen peroxide-induced apoptosis in S. cerevisiae. Cell 120, 25-36.

Ahn, S.H., Henderson, K.A., Keeney, S., Allis, C.D. (2005b). H2B (Ser10) phosphorylation is induced during apoptosis and meiosis in S. cerevisiae. Cell Cycle 4, 780-783.

Aylon, Y., Oren, M. (2011). p53: Guardian of ploidy. Mol. Oncol. [Epub ahead of print]

Barr, F.A., Gruneberg, U. (2007). Cytokinesis: placing and making the final cut. Cell 131, 847-860.

Becker, W., Weber, Y., Wetzel, K., Eirmbter, K., Tejedor, F.J., Joost, H.G. (1998). Sequence characteristics, subcellular localization, and substrate specificity of DYRK-related kinases, a novel family of dual specificity protein kinases. J. Biol. Chem. 273, 25893-25902.

Bleher, R., Martin, R. (1999). Nucleo-cytoplasmic translocation of histone H1 during the HeLa cell cycle. Cromosoma 108, 308-316.

Bracaglia, G., Conca, B., Bergo, A., Rusconi, L., Zhou, Z., Greenberg, M.E., Landsberger, N., Soddu, S., Kilstrup-Nielsen, C. (2009). Methyl-CpG-binding protein 2 is phosphorylated by homeodomain-interacting protein kinase 2 and contributes to apoptosis. EMBO Rep. 10, 1327-1333.

Calzado, M.A., Renner, F., Roscic, A., Schmitz, M.L. (2007). HIPK2: a versatile switchboard regulating the transcription machinery and cell death. Cell Cycle. 6, 139-143.

Calzado, M.A., de la Vega, L., Mö ller, A., Bowtell, D.D., Schmitz, M.L. (2009). An inducible autoregulatory loop between HIPK2 and Siah2 at the apex of the hypoxic response. Nat. Cell Biol. 11, 85-91.

Castedo, M., Coquelle, A., Vivet, S., Vitale, I., Kauffmann, A., Dessen, P., Pequignot, M.O., Casares, N., Valent, A., Mouhamad, S., et al. (2006). Apoptosis regulation in tetraploid cancer cells. EMBO J. 25, 2584-2595.

Cheung, P., Allis, C.D., Sassone-Corsi, P. (2000). Signaling to chromatin through histone modifications. Cell 103, 263-271.

Cheung, W.L., Ajiro, K., Samejima, K., Kloc, M., Cheung, P., Mizzen, C.A., Beeser, A., Etkin, L.D., Chernoff, J., Earnshaw, W.C., Allis, C.D. (2003). Apoptotic phosphorylation of histone H2B is mediated by mammalian sterile twenty kinase. Cell 113, 507-517.

Cimini, D., Mattiuzzo, M., Torosantucci, L., and Degrassi, F. (2003). Histone hyperacetylation in mitosis prevents sister chromatid separation and produces chromosome segregation defects. Mol. Biol. Cell 14, 3821–3833.

D'Orazi, G., Cecchinelli, B., Bruno, T., Manni, I., Higashimoto, Y., Saito, S., Gostissa, M., Coen, S., Marchetti, A., Del Sal, G., Piaggio, G., Fanciulli, M., Appella, E., Soddu, S. (2002). Homeodomain-interacting protein kinase-2 phosphorylates p53 at Ser 46 and mediates apoptosis. Nat. Cell Biol. 4, 11-19.

Fujiwara, T., Bandi, M., Nitta, M., Ivanova, E.V., Bronson, R.T., Pellman, D. (2005). Cytokinesis failure generating tetraploids promotes tumorigenesis in p53-null cells. Nature 437, 1043-1047.

Ganem, N.J., Storchova, Z., Pellman, D. (2007). Tetraploidy, aneuploidy and cancer. Curr. Opin. Genet. Dev. 17, 157-162.

Glotzer, M. (2005). The Molecular Requirements for Cytokinesis. Science 307, 1735-1739.

Gresko, E., Ritterhoff, S., Sevilla-Perez, J., Roscic, A., Frobius, K., Kotevic, I., Vichalkovski, A., Hess, D., Hemmings, B.A., Schmitz, M.L. (2009). PML tumor suppressor is regulated by HIPK2-mediated phosphorylation in response to DNA damage. Oncogene 28, 698-708.

Guizetti, J., Gerlich, D.W. (2010) Cytokinetic abscission in animal cells. Semin. Cell Dev. Biol. 21, 909-916.

Haglund, K., Nezis, I.P., Stenmark, H. (2011). Structure and functions of stable intercellular bridges formed by incomplete cytokinesis during development. Commun. Integr. Biol. 4, 1-9.

Hikasa, H., Ezan, J., Itoh, K., Li, X., Klymkowsky, M.W., Sokol, S.Y. (2010). Regulation of TCF3 by Wnt-dependent phosphorylation during vertebrate axis specification. Dev. Cell 19, 521-32.

Hofmann, T.G., Mö ller, A., Sirma, H., Zentgraf, H., Taya, Y., Drö ge, W., Will, H., Schmitz, M.L. (2002). Regulation of p53 activity by its interaction with homeodomain-interacting protein kinase-2. Nat. Cell Biol. 4, 1-10.

Isono, K., Nemoto, K., Li, Y., Takada, Y., Suzuki, R., Katsuki, M., Nakagawara, A., Koseki, H. (2006). Overlapping roles for homeodomain-interacting protein kinases hipk1 and hipk2 in the mediation of cell growth in response to morphogenetic and genotoxic signals. Mol. Cell Biol. 26, 2758-2771.

Kanei-Ishii, C., Ninomiya-Tsuji, J., Tanikawa, J., Nomura, T., Ishitani, T., Kishida, S., Kokura, K., Kurahashi, T., Ichikawa-Iwata, E., Kim, Y., Matsumoto, K., Ishii, S. (2004). Wnt-1 signal induces phosphorylation and degradation of c-Myb protein via TAK1, HIPK2, and NLK. Genes Dev. 18, 816-829.

Kim, Y.H., Choi, C.Y., Lee, S.J., Conti, M.A., Kim, Y. (1998). Homeodomain-interacting protein kinases, a novel family of co-repressors for homeodomain transcription factors. J. Biol. Chem. 273, 25875-25879.

Kim, E.J., Park, J.S., Um, S.J. (2002). Identification and characterization of HIPK2 interacting with p73 and modulating functions of the p53 family in vivo. J. Biol. Chem. 277, 32020- 32028.

Kimura, H., Cook, P.R. (2001). Kinetics of core histones in living human cells: little exchange of H3 and H4 and some rapid exchange of H2B. J. Cell Biol. 153, 1341-1353.

Kobiyama, K., Takeshita, F., Jounai, N., Sakaue-Sawano, A., Miyawaki, A., Ishii, K.J., Kawai, T., Sasaki, S., Hirano, H., Ishii, N., et al. (2010). Extrachromosomal histone H2B mediates innate antiviral immune responses induced by intracellular double-stranded DNA. J. Virol. 84; 822-832.

Konishi, A., Shimizu, S., Hirota, J., Takao, T., Fan, Y., Matsuoka, Y., Zhang, L., Yoneda, Y., Fujii, Y., Skoultchi, A.I., Tsujimoto, Y. (2003). Involvement of histone H1.2 in apoptosis induced by DNA double-strand breaks. Cell 114, 673-688.

Krieghoff-Henning, E., Hofmann, T.G. (2008). HIPK2 and cancer cell resistance to therapy. Future Oncol. 4, 751-754.

Kuriyama, R., Keryer, G., Borisy, G.G. (1984). The mitotic spindle of Chinese hamster ovary cells isolated in taxol-containing medium. J. Cell Sci. 66, 265-275.

Lavra, L., Rinaldo, C., Ulivieri, A., Luciani, E., Fidanza, P., Giacomelli, L., Bellotti, C., Ricci, A., Trovato, M., Soddu, S., et al. (2011). The Loss of the p53 Activator HIPK2 Is Responsible for Galectin-3 Overexpression in Well Differentiated Thyroid Carcinomas. PLoS One 6, 20665.

Lazzari, C., Prodosmo, A., Siepi, F., Rinaldo, C., Galli, F., Gentileschi, M., Bartolazzi, A., Costanzo, A., Sacchi, A., Guerrini, L., Soddu, S. (2011). HIPK2 phosphorylates ΔNp63α and promotes its degradation in response to DNA damage. Oncogene [Epub ahead of print]

Li, X.L., Arai, Y., Harada, H., Shima, Y., Yoshida, H., Rokudai, S., Aikawa, Y., Kimura, A., Kitabayashi, I. (2007). Mutations of the HIPK2 gene in acute myeloid leukemia and myelodysplastic syndrome impair AML1- and p53-mediated transcription. Oncogene 26, 7231-7239.

Li, Q., Lin, S., Wang, X., Lian, G., Lu, Z., Guo, H., Ruan, K., Wang, Y., Ye, Z., Han, J., Lin, S.C. (2009). Axin determines cell fate by controlling the p53 activation threshold after DNA damage. Nat. Cell Biol. 11, 1128-1134.

Lodola, A., Almouzni, G. (2004). Histone chaperones, a supporting role in the limelight. Biochim. Biophys. Acta. 1677, 3-11.

Mao, J.H., Wu, D., Kim, I.J., Kang, H.C., Wei, G., Climent, J., Kumar, A., Pelorosso, F.G., Delrosario, R., Huang, E.J., Balmain, A. (2011). Hipk2 cooperates with p53 to suppress γ-ray radiation-induced mouse thymic lymphoma. Oncogene [Epub ahead of print]

Mecklenbrä uker, I., Kalled, S.L., Leitges, M., Mackay, F., Tarakhovsky, A. (2004). Regulation of B-cell survival by BAFF-dependent PKCdelta-mediated nuclear signalling. Nature 431, 456-461.

Normand, G., King, R.W. (2010). Understanding citokinesis failure. Adv. Exp. Med. Biol. 676, 27-55.

Pérez-Cadahía, B., Drobic, B., Khan, P., Shivashankar, C.C., Davie, J.R. (2010). Current understanding and importance of histone phosphorylation in regulating chromatin biology. Curr. Opin. Drug Discov. Devel. 13, 613-622.

Pierantoni, G.M., Rinaldo, C., Mottolese, M., Di Benedetto, A., Esposito, F., Soddu, S., Fusco, A. (2007). High-mobility group A1 inhibits p53 by cytoplasmic relocalization of its proapoptotic activator HIPK2. J. Clin. Invest. 17, 693-702.

Puca, R., Nardinocchi, L., Givol, D., D'Orazi, G. (2010). Regulation of p53 activity by HIPK2: molecular mechanisms and therapeutical implications in human cancer cells. Oncogene 29, 4378-4387.

Rinaldo, C., Prodosmo, A., Siepi, F., Soddu, S. (2007a). HIPK2: a multitalented partner for transcription factors in DNA damage response and development. Biochem. Cell. Biol. 85, 411-418.

Rinaldo, C., Prodosmo, A., Mancini, F., Iacovelli, S., Sacchi, A., Moretti, F., Soddu, S. (2007b). MDM2-regulated degradation of HIPK2 prevents p53Ser46 phosphorylation and DNA damage-induced apoptosis. Mol. Cell 25, 739-750.

Ritterhoff, S., Farah, C.M., Grabitzki, J., Lochnit, G., Skurat, A.V., Schmitz, M.L. (2010). The WD40-repeat protein Han11 functions as a scaffold protein to control HIPK2 and MEKK1 kinase functions. EMBO J. 29, 3750-3761.

Roscic, A., Mö ller, A., Calzado, M.A., Renner, F., Wimmer, V.C., Gresko, E., Lü di, K.S., Schmitz, M.L. (2006). Phosphorylation-dependent control of Pc2 SUMO E3 ligase activity by its substrate protein HIPK2. Mol Cell 24, 77-89.

Ruchaud, S., Carmena, M., Earnshaw, W.C. (2007). Chromosomal passengers: conducting cell division. Nat. Rev. Mol. Cell Biol. 8, 798-812.

Rui, Y., Xu, Z., Lin, S., Li, Q., Rui, H., Luo, W., Zhou, H.M., Cheung, P.Y., Wu, Z., Ye, Z., et al. (2004). Axin stimulates p53 functions by activation of HIPK2 kinase through multimeric complex formation. EMBO J. 23, 4583-4594.

Saxton, W.M., McIntosh, J.R. (1987). Interzone microtubule behavior in late anaphase and telophase spindles. J. Cell Biol.105, 875-886.

Shima, Y., Shima, T., Chiba, T., Irimura, T., Pandolfi, P.P., Kitabayashi, I. (2008). PML activates transcription by protecting HIPK2 and p300 from SCFFbx3-mediated degradation. Mol. Cell. Biol. 28, 7126-7138.

Skop, A.R., Liu, H., Yates, J. 3rd, Meyer, B.J., Heald, R. (2004). Dissection of the mammalian midbody proteome reveals conserved cytokinesis mechanisms. Science 305, 61-66.

Song, L., Li, D., Liu, R., Zhou, H., Chen, J., Huang, X. (2007). Ser-10 phosphorylated histone H3 is involved in cytokinesis as a chromosomal passenger. Cell Biol. Int. 31, 1184-1190.

Steigemann, P., Gerlich, D.W. (2009). Cytokinetic abscission: cellular dynamics at the midbody. Trends Cell Biol. 19, 606-616.

Steigemann, P., Wurzenberger, C., Schmitz, M.H., Held, M., Guizetti, J., Maar, S., Gerlich, D.W. (2009). Aurora B-mediated abscission checkpoint protects against tetraploidization. Cell 136, 473-484.

Swarup, S., Verheyen, E.M. (2011). Drosophila homeodomain-interacting protein kinase inhibits the Skp1-Cul1-F-box E3 ligase complex to dually promote Wingless and Hedgehog signaling. Proc. Natl. Acad. Sci. USA 108, 9887-9892.

Trapasso, F., Aqeilan, R.I., Iuliano, R., Visone, R., Gaudio, E., Ciuffini, L., Alder, H., Paduano, F., Pierantoni, G.M., Soddu, S., et al. (2009). Targeted disruption of

the murine homeodomain-interacting protein kinase-2 causes growth deficiency in vivo and cell cycle arrest in vitro. DNA Cell Biol. 28, 161-167.

Uetake, Y., Sluder, G. (2004). Cell cycle progression after cleavage failure: mammalian somatic cells do not possess a "tetraploidy checkpoint". J. Cell Biol. 165, 609-615.

Wee, H.J., Voon, D.C., Bae, S.C., Ito, Y. (2008). PEBP2-beta/CBF-beta-dependent phosphorylation of RUNX1 and p300 by HIPK2: implications for leukemogenesis. Blood 112, 3777-3787.

Wiggins, A.K., Wei, G., Doxakis, E., Wong, C., Tang, A.A., Zang, K., Luo, E.J., Neve, R.L., Reichardt, L.F., Huang, E.J. (2004). Interaction of Brn3a and HIPK2 mediates transcriptional repression of sensory neuron survival. J. Cell Biol. 167, 257-267.

Zhang, Q., Yoshimatsu, Y., Hildebrand, J., Frisch, S.M., Goodman, R.H. (2003). Homeodomain interacting protein kinase 2 promotes apoptosis by downregulating the transcriptional corepressor CtBP. Cell 115, 177-186.

Zhang, Q., Wang, Y. (2007). Homeodomain-interacting protein kinase-2 (HIPK2) phosphorylates HMGA1a at Ser-35, Thr-52, and Thr-77 and modulates its DNA binding affinity. J. Proteome Res. 6, 4711-4719.